CAPITAL UNIVERSITY OF SCIENCE AND TECHNOLOGY, ISLAMABAD

Evaluating the Role of Etoricoxib in Attenuating Inflammation in Ethanol-Induced Hepatotoxicity

by

Aqeela Khurshid

A thesis submitted in partial fulfillment for the degree of Master of Philosophy

in the

Faculty of Pharmacy
Department of Pharmacology

2025

I wholeheartedly dedicate this work to my beloved parents and respected teachers, whose prayers, encouragement, and inspiring words have guided me throughout. I am equally grateful to my family and sincere well-wishers, whose love, sacrifices, and unwavering support have been the strength behind every step of my journey and their lives teach me how to step forward.

CERTIFICATE OF APPROVAL

Evaluating the Role of Etoricoxib in Attenuating Inflammation in Ethanol-Induced Hepatotoxicity

by

Aqeela Khurshid

(MPH233008)

THESIS EXAMINING COMMITTEE

S. No.	Examiner	Name	Organization
(a)	External Examiner	Dr. Aslam Khan	RIU, Islamabad
(b)	Internal Examiner	Dr. Muzaffar Abbas	CUST, Islamabad
(c)	Supervisor	Dr. Fazlullah Khan	CUST, Islamabad

Dr. Fazlullah Khan
Thesis Supervisor
October, 2025

Dr. Fazlullah Khan
Head
Department of Pharmacy
October, 2025

Dr. Muzaffar Abbas
Dean
Faculty of Pharmacy
October, 2025

Author's Declaration

I, **Aqeela Khurshid** hereby state that my MS thesis titled "**Evaluating the Role of Etoricoxib in Attenuating Inflammation in Ethanol-Induced Hepatotoxicity**" is my own work and has not been submitted previously by me for taking any degree from Capital University of Science and Technology, Islamabad or anywhere else in the country/abroad.

At any time if my statement is found to be incorrect even after my graduation, the University has the right to withdraw my MPhill Degree.

(Aqeela Khurshid)

Registration No: MPH233008

Plagiarism Undertaking

I solemnly declare that research work presented in this thesis titled "**Evaluating the Role of Etoricoxib in Attenuating Inflammation in Ethanol-Induced Hepatotoxicity**" is solely my research work with no significant contribution from any other person. Small contribution/help wherever taken has been duly acknowledged and that complete thesis has been written by me.

I understand the zero tolerance policy of the HEC and Capital University of Science and Technology towards plagiarism. Therefore, I as an author of the above titled thesis declare that no portion of my thesis has been plagiarized and any material used as reference is properly referred/cited.

I undertake that if I am found guilty of any formal plagiarism in the above titled thesis even after award of MPhill Degree, the University reserves the right to withdraw/revoke my MPhill degree and that HEC and the University have the right to publish my name on the HEC/University website on which names of students are placed who submitted plagiarized work.

(Aqeela Khurshid)

Registration No: MPH233008

Acknowledgement

In the name of Allah, the Most Gracious, the Most Merciful. All praise is due to Allah, the Lord of the worlds. With a heart full of humility and gratitude, I begin by offering my eternal thanks to Almighty Allah (SWT), the ultimate source of knowledge, patience, and strength. I send peace and blessings upon our beloved Prophet Muhammad (PBUH), whose life remains a radiant beacon of faith, whose teachings of compassion, knowledge, and perseverance continue to illuminate the path for seekers of truth and knowledge around the world.

I am profoundly grateful to my distinguished supervisor, Dr. Fazlullah khan, Associate Professor, His insightful mentorship, inspiring leadership, and constant encouragement elevated the quality of my work and nurtured my growth as a researcher. I extend heartfelt thanks to Prof Dr. Muzaffar Abbas, Dean of faculty of pharmacy, whose support, both academic and personal, helped shape this endeavour and made the environment at CUST rich with knowledge and encouragement. To respected Mr. M. Ibrar Khan your guidance and support have been a true blessing in my academic path. I am also deeply grateful to Mr. Sardar Usman Sarosh for his constant encouragement, thoughtful guidance, and sincere support throughout this journey.

To my colleagues Ms. Ibtisam Zakir, Ms. Sadia Khaliq, Ms. Tuba Naseer, Ms. Iqra Nawaz, Ms. Asma Jabeen thank you for your companionship, your valuable insights, and for turning this rigorous path into a collaborative. I extend my deepest gratitude to my family, the foundation of all my achievements. To my father, whose strength, wisdom, and unwavering belief shaped my journey, and to my mother, whose boundless love, prayers, and sacrifices sustained me through every challenge. I owe everything to you both. Their silent support and selfless devotion are behind every success. I am also thankful to all who offered kind words, prayers, and support along the way; your presence made a lasting impact.

(Aqeela Khurshid)

Abstract

Ethanol-induced hepatotoxicity is a significant clinical and public health concern due to oxidative stress, immune dysfunction, and persistent chronic inflammation that sustain liver injury. Cyclooxygenase-2 (COX-2) is an important mediator of liver inflammation through the formation of pro-inflammatory prostaglandins and activation of NF-κB. Etoricoxib selective COX-2 inhibitor offers a therapeutic modality that has no gastrointestinal side-effects. In this study, we examined the hepatoprotective effects of etoricoxib compared to ibuprofen, a non-selective COX inhibitor, in an animal model of ethanol-induced hepatotoxicity. Hepatotoxicity was induced with ethanol 20% v/v (5 g/kg), i.p. for 9 consecutive days. The treatment groups received low dose etoricoxib (25 mg/kg), high dose etoricoxib (50 mg/kg), ibuprofen (50 mg/kg) for 9 days. Upon completion of the treatment period blood samples were taken and liver injury was assessed with biochemical measures of ALT, AST, and protein content (BCA assay) as well as pro-inflammatory cytokines TNF-α using ELISA. The results from the follow up blood sample analysis following the completion of the ethanol protocol demonstrated significantly increased serum levels of ALT, AST and TNF-α in the mice that were challenged with ethanol alone, indicating acute liver injury. In regards to etoricoxib (50 mg/kg) treatment had significantly reduced liver damage markers compared to both etoricoxib (25 mg/kg) and ibuprofen treatments ($p< 0.05$). Additionally, molecular docking analysis demonstrated strong binding affinities of etoricoxib to pro-inflammatory targets; COX-2 (-10.5 kcal/mol), TNF-α (-9.2 kcal/mol), and NF-κB (-8.7 kcal/mol), suggesting a multi-target mechanism underlying its anti-inflammatory and hepatoprotective actions. These findings collectively demonstrate that etoricoxib, particularly at a dose of (50 mg/kg), offers significant protection against ethanol-induced liver injury through attenuation of oxidative stress and inflammation, outperforming both the lower dose of etoricoxib and ibuprofen. This highlights its potential as a safer and more effective alternative for managing ethanol-related hepatic inflammation. These preliminary findings suggest that etoricoxib could potentially be used to treat ethanol-induced liver injury.

Contents

Author's Declaration iv

Plagiarism Undertaking v

Acknowledgement vi

Abstract vii

List of Figures xi

List of Tables xiii

Abbreviations xiv

Symbols xvi

1 Introduction 1

1.1 Background . . . 1
1.2 Ethanol as Hepatotoxic Agent . . . 2
1.3 Pathophysiology of Liver Damage . . . 2
1.3.1 Hepatic Steatosis . . . 2
1.3.2 Alcoholic Hepatitis . . . 3
1.3.3 Hepatic Fibrosis . . . 3
1.3.4 Liver Cirrhosis . . . 5
1.3.5 Hepatotoxicity . . . 5
1.3.5.1 Acute Ethanol Hepatotoxicity . . . 6
1.3.5.2 Sub-acute Ethanol Toxicity . . . 6
1.4 Ethanol Metabolism . . . 6
1.4.1 Alcohol Deydrogenase . . . 7
1.4.2 Cytochrome-P450 CYP2E1 Enzyme . . . 8
1.4.3 Aldehyde Dehydrogenase . . . 9
1.4.4 Catalase . . . 9
1.5 Ethanol Induced ROS Production . . . 9
1.6 Cyclooxygenase-2 Pathway . . . 11
1.7 COX-2 as a Therapeutic Target . . . 12
1.8 Therapeutic Role of Ibuprofen . . . 13

2 Literature Review **14**
2.1 Introduction . . . 14
2.2 Aims and Objectives . . . 20

3 Materials and Methods **21**
3.1 Introduction . . . 21
3.2 Ethical Statement . . . 23
3.3 Experimental Animal . . . 24
3.3.1 Food Composition . . . 24
3.3.2 Mice Bedding . . . 24
3.3.3 Animal Handling . . . 25
3.4 Grouping and Experimental Design . . . 26
3.4.1 Grouping of Mice . . . 27
3.5 Routes of Administration . . . 29
3.5.1 Intraperitoneal Route of Drug Administration . . . 29
3.6 Chemicals . . . 30
3.6.1 Drug Solubility . . . 30
3.6.2 Drug Preparation . . . 31
3.6.2.1 Dose Calculations for Ethanol 20% v/v (5g/kg) . . . 31
3.6.2.2 Dose Calculations Etoricoxib (25 mg/kg), Etoricoxib (50mg / kg), (Ibuprofen 50mg/kg) . . . 31
3.6.3 Dosing Protocol . . . 32
3.7 Personal Protective Equipment and Biosafety Measures . . . 34
3.8 Euthanasia and Methods of Euthanasia . . . 34
3.8.1 Methods of Euthanasia Fall into Categories Physical Method and Chemical Method . . . 35
3.8.1.1 Chemical Method . . . 35
3.9 Blood Withdrawal Techniques . . . 36
3.9.1 Cardiac Puncture . . . 37
3.9.2 Blood Withdrawal By Cardiac Puncture Procedure . . . 38
3.10 Dissection and Liver Preservation . . . 39
3.10.1 Extraction of Liver . . . 39
3.11 Biochemical Analysis . . . 40
3.11.1 Liver Homogenate Preparation . . . 40
3.11.1.1 Preparation of 0.1% Tween 80 PBS buffer 7.4 . . . 41
3.11.2 BCA Protein Assay Protocol . . . 41
3.11.2.1 Liver Tissue Collection and Preparation . . . 42
3.11.3 ELISA Test . . . 44
3.11.3.1 Assay Procedure . . . 44
3.12 Molecular Docking . . . 45
3.12.1 Ligands Preparation . . . 46
3.12.2 Proteins Preparation . . . 47
3.13 Evaluation of Liver Histopathological Changes . . . 48
3.14 Statistical Analysis . . . 49

4 Results **50**
4.1 Biochemical Markers of Hepatic Injury 50
4.2 Serum Alanine Aminotransferase and Serum Aspartate Aminotransferase Levels 51
4.3 Inflammatory Marker Analysis 54
4.3.1 BCA Protein Assay Protocol 54
4.3.2 TNF-α levels 56
4.3.2.1 TNF-α Levels in Experimental Groups 56
4.4 Molecular Docking Analysis 59
4.4.1 Molecular Docking Analysis of Etoricoxib Compound at Different Cytokines Receptor 59
4.4.2 Molecular Docking Analysis of Ibuprofen Compound at Different Cytokines Receptor 62
4.5 Histopathological Changes in Ethanolic Liver Injury due to Etoricoxib Administration 65

5 Discussion **67**
5.1 Limitations 74

6 Conclusion and Future Work **75**
6.1 Future Prospective 78

Bibliography **82**

List of Figures

1.1 Hepatic fibrosis progression leads to chronic liver cirrhosis. 4
1.2 Ethanol metabolism by ADH cyclic pathway. 7
1.3 Ethanol metabolism elevates mitochondrial ROS, causing oxidative stress. 11
1.4 Ethanol metabolism and ROS production leads to inflammation. . . 12

3.1 Experimental study design representing the *in vivo* study protocol in Ethanol-Induced Hepatotoxicity. 23
3.2 Animal handling using standardized tail and scruff handling techniques to minimize stress. 25
3.3 Mice were acclimatized to animal facility conditions prior to the commencement of experimental study. 26
3.4 Mice identification and marking protocol for experimental studies. . 27
3.5 Randomization strategy for experimental grouping of mice (n = 6 per group). 28
3.6 I.P. Injection in the lower right abdominal quadrant of mice. 29
3.7 Daily body weight measurement of mice. 32
3.8 Classification of euthanasia techniques. 35
3.9 Blood withdrawal techniques in mice. 36
3.10 Blood withdrawal by cardiac puncture. 37
3.11 Tubes used for blood collection from mice. 38
3.12 Liver collection and biochemical analysis. 40
3.13 Use of a microplate reader to analyze BCA protein assay. 43
3.14 Primary coated antibody 96 well plates used in ELISA assay. 45

4.1 Serum alanine transaminase levels in ethanol-induced liver injury in mice. 53
4.2 Serum aspartate transaminase levels in ethanol-induced liver injury in mice. 53
4.3 BCA assay, protein concentration in experimental group. 55
4.4 Standard curve for TNF-α. 56
4.5 TNF-α concentration in experimental group by ELSIA. 57
4.6 3D and 2D visualization of interaction with amino acid residues of the COX-2 active site with ligand etoricoxib. 59
4.7 3D and 2D visualization of interaction with amino acid residues of the TNF-α active site with ligand etoricoxib. 60

4.8 3D and 2D visualization of interaction with amino acid residues of the NF-κB active site with ligand etoricoxib. 61
4.9 3D and 2D visualization of interaction with amino acid residues of the COX-2 active site with ligand ibuprofen. 63
4.10 3D and 2D visualization of interaction with amino acid residues of the COX-2 active site with ligand ibuprofen. 63
4.11 3D and 2D visualization of interaction with amino acid residues of the NF-κB active site with ligand ibuprofen. 64
4.12 Hematoxylin and eosin staining of cross-sectional liver tissue across experimental 66

6.1 Comparative mechanistic overview of Etoricoxib and Ibuprofen in ethanol-induced hepatotoxicity. 77

List of Tables

3.1 Composition of animal food 24
3.2 Experimental groups and treatments description 28
3.3 List of equipments 30
3.4 Daily treatment schedule and observations for all experimental groups 33
3.5 List of PPEs 34
3.6 Material required for blood collection 37
3.7 Chemicals required for PBS buffer 7.4 41
3.8 Materials required for BCA assay 41

4.1 Binding affinities of etoricoxib with receptors 59
4.2 Binding affinities of ibuprofen with receptors 62

Abbreviations

ADH	Alcohol Dehydrogenase
ALDH	Aldehyde Dehydrogenase
ALT	Alanine Aminotransferase
ANOVA	Analysis of Variance
AST	Aspartate Aminotransferase
AVMA	American Veterinary Medical Association
BCA	Bicinchoninic Acid (protein assay)
cAMP	Cyclic Adenosine Monophosphate
CAT	Catalase
COX	Cyclooxygenase
COX-2	Cyclooxygenase-2
DALY	Disability-Adjusted Life Year
DAMP	Damage-Associated Molecular Patterns
DMSO	Dimethyl Sulfoxide
ELISA	Enzyme-Linked Immunosorbent Assay
EP2/EP4	Prostaglandin E2 Receptors
HSCs	Hepatic Stellate Cells
IACUC	Institutional Animal Care and Use Committee
IL-1β	Interleukin-1 beta
IL-6	Interleukin-6
IP	Intraperitoneal
IV	Intravenous
LPS	Lipopolysaccharide
MEOS	Microsomal Ethanol Oxidizing System

NF-κB	Nuclear Factor kappa-light-chain-enhancer of activated B cells
NSAID	Non-Steroidal Anti-Inflammatory Drug
PBS	Phosphate Buffered Saline
PDGF-β	Platelet-Derived Growth Factor-beta
PGE_2	Prostaglandin E2
PGT	Prostaglandin Transporter
PPE	Personal Protective Equipment
PRR	Pattern Recognition Receptors
ROS	Reactive Oxygen Species
SC	Subcutaneous
SD	Standard Deviation
TGF-β	Transforming Growth Factor-beta
TNF-α	Tumor Necrosis Factor Alpha

Symbols

α	Alpha
CH_3CHOH	1-hydroxyethyl radical
$CHCl_3$	Chemical formula for chloroform
C_2H_5OH	Chemical formula for ethanol
^oC	Degree Celsius
g/kg	Grams per kilogram
H_2O_2	Hydrogen peroxide
$HO\cdot$	Hydroxyl radical
μg/μL	Microgram per microliter
μL	Microliter
mg/kg	Milligrams per kilogram
NAD^+	Nicotinamide adenine dinucleotide
NADH	Nicotinamide adenine dinucleotide
$O_2\cdot^-$	Superoxide anion
U/L	Units per liter
Zn^{2+}	Zinc ion

Chapter 1

Introduction

1.1 Background

The liver is the largest internal gland and one of the most vital organs in the human body, performing a wide range of physiological functions necessary for sustaining life [1, 2]. As the body's primary metabolic hub, it has ability to detoxify various metabolites. Liver play significant role in metabolism, detoxification, digestion, and immune system defense [3].The liver has a key role in regulating immunity and is home to resident macrophages and specialized immune cells called Kupffer cells that are needed for removing debris and infection from the bloodstream [4, 5]. Liver is able to serve as a first line defense against pathogens and toxins ingested due to its position between the gastrointestinal tract and the systemic circulation [6]. The liver is vulnerable to damage due to prolonged exposure to toxic chemicals such as alcoholdrug and industrial toxins. Chronic alcohol consumption can lead to conditions ranging from steatosis to alcoholic hepatitis cirrhosis and liver failure. Toxic substances cause direct hepatocellular injury, oxidative stress, inflammation and disrupt mitochondrial function, all of which impair liver health and performance [7]. Long-term or repeated exposure to such substances overwhelms the liver's detoxification systems, leads to the buildup of reactive oxygen species (ROS), oxidative damage to lipids, activation of inflammatory pathways, and ultimately, cellular death [8].

The liver biochemical markers considered to be the most sensitive and specific to liver injury, are Alanine aminotransferase (ALT) and aspartate aminotransferase (AST). ALT is a cytosolic enzyme located in hepatocytes and is thus more liver specific than AST. An elevation of ALT in serum is reflective of hepatocellular injury of, especially due to hepatotoxic materials and liver inflammation [9].

1.2 Ethanol as Hepatotoxic Agent

Ethanol exists as a colorless and volatile liquid with the molecular formula C_2H_5OH [10]. Ethanol rank among most widely abused psychoactive substances worldwide [11]. Ethanol is a widely used substance with significant physiological, medical, and social implications. Excessive ethanol intake is a major global public health concern, a well-established contributor to early-onset disease and increased mortality [12]. As per the World Health Organization, alcohol-related liver diseases are among the most damaging and lethal effects of alcohol abuse, particularly in groups with high and prolonged use.

Chronic and excessive ethanol consumption has severe implications on multiple organ systems, but ethanol metabolize in liver, rendering it highly susceptible to damage [13]. Ethanol is a small, amphiphilic molecule metabolized almost exclusively in the liver. Long-term ethanol consumption results in significant hepatocellular toxicity as a result of the accumulation of metabolites and production of ROS [14]. Ethanol induced liver injury has a characteristically orderly progression ranging from steatosis to alcoholic hepatitis to cirrhosis, fibrosis and hepatotoxicity [15].

1.3 Pathophysiology of Liver Damage

1.3.1 Hepatic Steatosis

Hepatic steatosis is characterized by lipids, predominantly triglycerides, phospholipids and cholesterol esters, accumulating in perivenular hepatocytes; it may later progress into the periportal region of the liver [16]. Ethanol is absorbed from the jejunum and small amounts of fat are also absorbed from the mouth, esophageal,

gastric, and large intestine mucosal membranes. Ethanol consumption, enhance the transport of fats from peripheral adipose tissue to the liver while simultaneously impairing fat export from the liver. The metabolism of ethanol alters the cellular NAD^+/NADH ratio toward a more reduced state in hepatocytes, inhibits fatty acid oxidation, lead to the subsequent accumulation of lipids and the development of hepatic steatosis. Ethanol metabolism elevates the NADH/NAD^+ ratio, which inhibits gluconeogenesis and fatty acid oxidation [16]. Ethanol-induced liver injury can evolve from steatohepatitis to fibrosis and cirrhosis, heightening the risk of fatal hepatic failure [17].

1.3.2 Alcoholic Hepatitis

Alcoholic hepatitis (AH) is marked by a decline in liver function, often presenting with symptoms like jaundice and portal hypertension. Characteristics of alcoholic hepatitis include severe steatohepatitis, jaundice, cholestatic liver injury, and a reduced ability for the liver to regenerate, all of which contribute to its notably high mortality rate. The inflammation in the liver caused by excessive ethanol intake is defined by damage to liver cells, by an influx of inflammatory cells, particularly polymorphonuclear leukocytes [18]. Polymorphonuclear leukocytes release pro-inflammatory cytokines tumor necrosis factor-alpha (TNF-α), interleukin-6 (IL-6), and interleukin-1β (IL-1β) in response to endotoxins that arise from increased gut permeability. The activity of CYP2E1 and mitochondrial dysfunction lead to the buildup of ROS, which worsen cellular damage and fuel inflammation [19, 20].

1.3.3 Hepatic Fibrosis

Liver fibrosis is a vascular and inherently dynamic disease process arising from the progressive deposition of extracellular matrix (ECM) proteins with subsequent structural disorganization and functional architecture that impairs the liver. The main cells drive, this process are hepatic stellate cells (HSCs), which undergo a phenotypic switch into myofibroblasts-like cells when they are activated by liver damage. In activated HSCs, proliferation, contractile, and fibrogenic properties

drive excess production of ECM proteins, especially type I collagen, major fibrillar collagen component of fibrotic liver tissues. An overproduction of ECM forms fibrotic parenchyma, largely replacing hepatocytic function and liver parenchyma stiffness. Specifically, PDGF-β receptor was identified as a key signal mediator of proliferation and migration in response to injury. Fibronectin is an ECM glycoprotein that is deposited early and promotes fibrosis by enhancing cell interaction with ECM during an injured, healing liver process. Alpha-Smooth Muscle Actin (α-SMA), the most distinguishing signature of myofibroblasts differentiation and indicates the contractile, synthetic phenotype of activated HSCs [21].

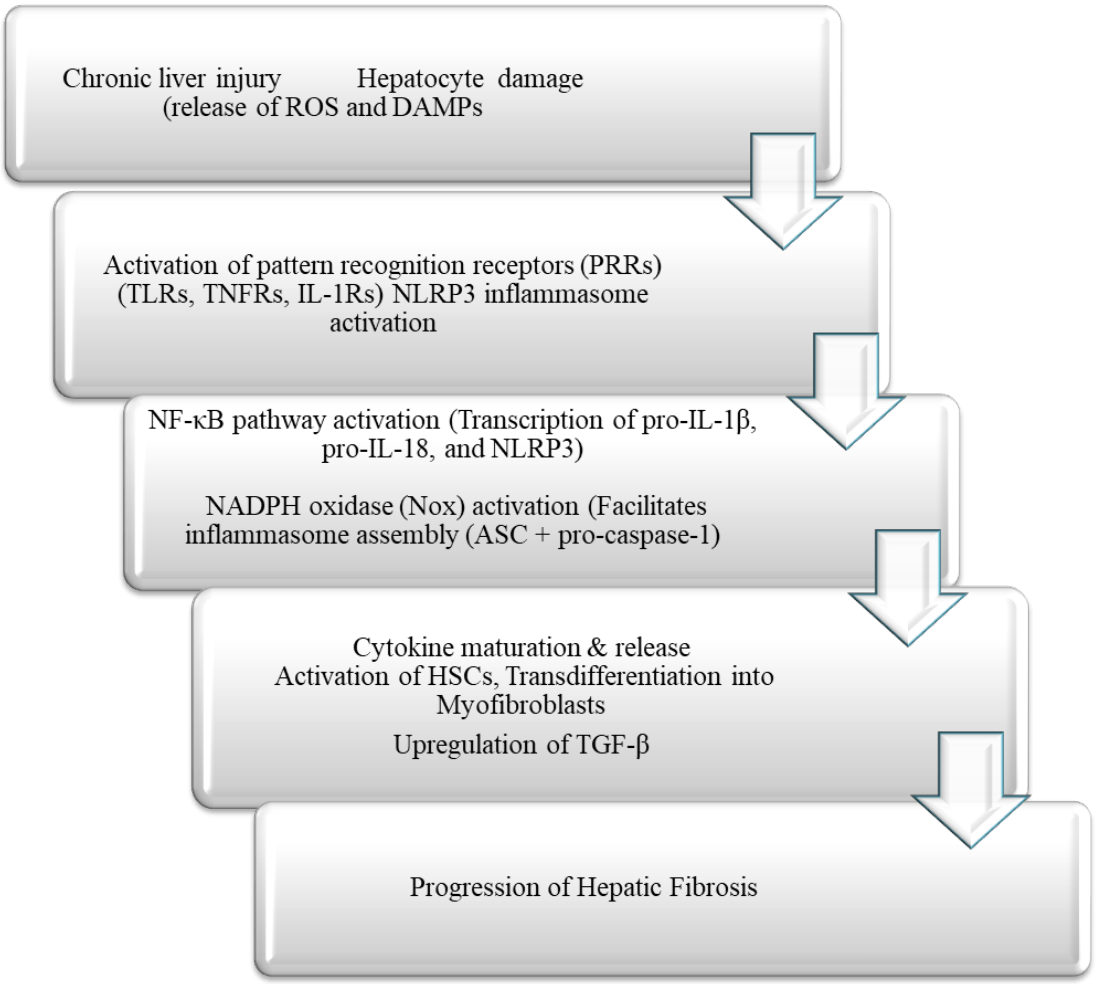

FIGURE 1.1: Hepatic fibrosis progression leads to chronic liver cirrhosis.

The above figure shows schematic representation of the pathological evolution of hepatic fibrosis into cirrhosis. The figure depicts the stages of liver injury, such as collagen deposition, nodular formation, and architectural distortion, which can

lead to cirrhosis in a "de-facto" irreversible course. There are several features of cirrhosis, including bridging fibrosis, regenerative nodules, and portal hypertension.

1.3.4 Liver Cirrhosis

Liver cirrhosis involves destruction of the liver parenchyma, often due to excessive alcohol consumption. It is a common condition characterized by fibrosis of the tissue and conversion of the liver's normal architecture into abnormal nodular formations. [22]. Cirrhosis of the liver is a disease that induces many irreversible morphological alterations, such as systemic fibrosis, regenerative nodules (altered hepatocytes), loss of normal lobular architecture, and abnormal anatomical vascular connections between the portal vein and hepatic artery.

Other structural factors such as sinusoidal capillarization, perisinusoidal fibrosis, thrombosis, obliterative vascular lesions disrupt blood flow to the parenchyma causing parenchymal hypoxia and liver dysfunction. The process of chronic necroinflammation induces the process of progressive fibrosis results in the activation of HSCs and a transition to myofibroblast-like cells.

These phenomena along with the excessive and dysregulated production of matrix metalloproteinase (MMPs) by activated HSCs overwhelm systemic synthesis of ECM components such as fibrillar collagens. In addition to HSC-related changes, Kupffer cells and invasive immune cells (monocytes and neutrophils), which also release large amounts of proinflammatory mediators causing destructive damage, inflammation, and fibrotic remodeling [23].

1.3.5 Hepatotoxicity

Ethanol induces liver damage mainly by disrupting redox balance due to excess NADH generation, during its breakdown via the alcohol dehydrogenase pathway. Additionally, it impairs the metabolism of key biomolecules, including lipids, carbohydrates, proteins, and purines.

1.3.5.1 Acute Ethanol Hepatotoxicity

Acute ethanol hepatotoxicity occurs when excess ethanol is consumed at a rate greater than the liver can process and eliminate, leading to accumulation of ethanol and its metabolites in the blood stream.

Intoxication is the result of this accumulation, and the signs and symptoms of acute alcohol intoxication vary from mild impairment of mental status, ataxia, and coordination and impairment of coordination to serious complications such as stupor, respiratory depression, or coma.

Alcohol amplifies CNS inhibition and decreases excitatory signals by working on gamma-amino butyric acid (GABA) receptors, which are the major CNS inhibitory chemicals [24].

1.3.5.2 Sub-acute Ethanol Toxicity

Sub-acute ethanol toxicity is liver damage due to repeated ingestion of excessive doses of ethanol over several days to weeks. It is not life-threatening as acute toxicity in that it causes cumulative physiological impairment. This change begins to interfere with organ function, including the liver, immune system, intestinal tract, metabolism in liver [25].

1.4 Ethanol Metabolism

In liver ethanol processes through number of key biochemical and enzymatic pathways including alcohol dehydrogenases (ADH), cytochrome P450 enzymes, the microsomal ethanol oxidizing system (MEOS), aldehyde dehydrogenases (ALDH) and catalase (CAT). Alcohol dehydrogenase class I (ADH1) is the principal enzyme responsible for ethanol metabolism. ADH1 accounts for approximately 80% of the ethanol metabolic rate with the remaining 20% attributed to non-ADH1 pathways [26].

1.4.1 Alcohol Deydrogenase

Ethanol metabolism is largely mediated by multiple isoforms of cytosolic alcohol dehydrogenases (ADHs). ADHs are zinc-dependent enzymes that facilitate the reversible conversion of primary and secondary alcohols into corresponding aldehydes and ketones. These ADHs are classified within the medium-chain dehydrogenase/reductase (MDR) superfamily, which catalyzes the oxidation of simple alcohols methanol and ethanol, into their respective aldehydes, formaldehyde and acetaldehyde, while reducing NAD+ to NADH [27]. ADHs participate in endogenous processes, such as the dehydrogenation of hydroxysteroids, the oxidation of intermediary alcohols, and the Omega-oxidation of fatty acid [26].

The catalytic cycle of ADH consists of several steps in ethanol oxidation.

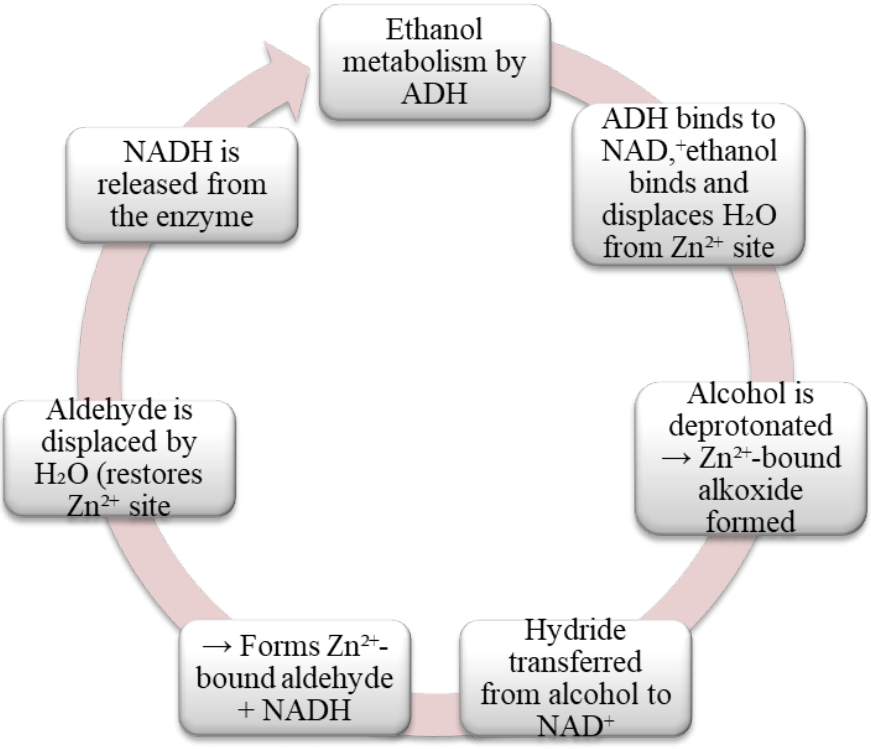

FIGURE 1.2: Ethanol metabolism by ADH cyclic pathway.

The above figure shows catalytic cycle of ADH-catalyzed oxidation of ethanol to acetaldehyde, reduction of NAD+ to NADH.

The cyclical pathway highlights the contribution of zinc ions (Zn^{2+}) in the active site and that the reaction is reversible leading to redox imbalance in hepatocytes.

ADH catalyzes the oxidation of ethanol to acetaldehyde through a well-orchestrated catalytic cycle involving the coenzyme NAD^+ and a zinc ion (Zn^{2+}) at the active site. The catalytic Zn2+ ion plays an important role by stimulating the deprotonation of the alcohol and accelerating the transfer of hydride to NAD+ during dehydrogenation.

In the reverse reaction (hydrogenation) Zn2+ increases the electrophilicity of the carbonyl carbon of aldehydes or ketones and allows for the conversion back to alcohols.

1.4.2 Cytochrome-P450 CYP2E1 Enzyme

A second major pathway of ethanol metabolism, the cytochrome P450 2E1 (CYP-2E1) pathway is the second major route of ethanol metabolism. This enzyme is predominantly expressed in the liver, particularly within the smooth endoplasmic reticulum of center lobular hepatocytes.

During CYP2E1 mediated ethanol metabolism, an unstable gem-diol intermediate forms and spontaneously breaks down into acetaldehyde. ROS generation, including the 1-hydroxyethyl radical, which contributes to oxidative stress.

ROS produced superoxide anion and hydrogen peroxide [28]. These ROS can further interact with transition metals (Fe^{2+}, Cu^+) via Fenton-like reactions, yielding highly reactive hydroxyl radicals.

Ethanol derived radicals, such as the hydroxyethyl radicals, form through one-electron oxidation of ethanol by superoxide at the CYP2E1 catalytic site. This reaction involves the ferric cytochrome P450-oxygen complex, further amplifying oxidative stress [29].

1.4.3 Aldehyde Dehydrogenase

Acetaldehyde dehydrogenase (ALDs) converts acetaldehyde to acetate. These enzymes use NAD+ as a cofactor during the oxidization of acetaldehyde. ADH isoenzymes play role in elimination of acetaldehyde, and also involve in detoxification of lipid peroxidation byproduct such as 4-hydroxynonenal (4-HNE) during oxidative stress [30].

1.4.4 Catalase

Catalases oxidize ethanol to acetaldehyde in H_2O_2-dependent manner. Catalases are considered as a minor pathway for ethanol metabolism. Catalase activity is dependent on the cellular concentration of H_2O_2. Under oxidative stress conditions, where H_2O_2 production is elevated, the capacity of catalases to metabolize ethanol may be enhanced [31].

1.5 Ethanol Induced ROS Production

The formation of ROS from the re-oxidation of NADH to NAD^+ in the mitochondria promotes liver injury from two mechanisms; oxidative damage, and indirect stimulation of lipid accumulation [32]. When hepatocyte injury occurs, these hepatocytes release DAMPs, several cytokines, and chemokines that lead to the recruitment and activation of innate immune cells specifically macrophages and neutrophils. Once activated, these cells accelerate the ROS formation primarily by NADPH oxidase (NOX). NOX is a multi-subunit enzyme complex that turns oxygen into superoxide as it uses NADPH as an electron donor [33].

ROS are highly reactive and can damage cellular components, including lipids, proteins, and nucleic acids. ROS react with lipids initiate lipid peroxidation, producing reactive aldehydes such as 4-hydroxynonenal (4-HNE) and MDA. Reactive aldehydes formed during metabolism of ethanol will form protein adducts, which can serve as neoantigens, and engage adaptive immune responses using T and B lymphocytes.

ROS are released from damaged hepatocytes, which can activate inflammatory cells to further drive inflammation and create a vicious cycle of oxidative stress through ROS and reactive nitrogen species (RNS), such as peroxynitrite ($ONOO^-$) and nitric oxide (NO), production before, and after injury by the inflammasome [34].

The liver resident macrophages, Kupffer cells (KCs) contribute to hepatic inflammation by secreting proinflammatory cytokines and chemokines. The released factors can recruit and mediate inflammation in circulating monocytes and macrophages [34].

ROS generated by NOX in activated macrophages signal through nuclear factor-kappa B (NF-κB) to drive TNF-α production in Kupffer cells [35]. Lipopolysaccharide (LPS) will bind to CD14 receptors on Kupffer cells, which can activate NF-κB and increase transcription of proinflammatory mediators TNF-α, COX-2, IL-6, and transforming growth factor-beta (TGF-β). These cytokines are key mediators in cholestasis and acute-phase protein synthesis. LPS and other inflammatory signals will initiate and rapidly activate the expression of inducible nitric oxide synthase (iNOS) and cyclooxygenase-2 (COX-2).

Cells that express both inducible prostaglandin endoperoxide synthase (PGHS) and nitric oxide synthase (NOS), nitric oxide (NO), potentiate the formation of prostaglandins. NF-κB involved in the induction of COX-2 expression in response to LPS stimulation in macrophages [36]. Oxidative stress is further amplified by the depletion of reduced glutathione (GSH), a critical antioxidant. ROS also sensitize Kupffer cells to LPS, which enhances TNF-α production. LPS binds to the CD14 receptor on Kupffer cells and activates NF-κB, which increases the transcription of several proinflammatory cytokines, including TNF-α, IL-6, and TGF-β.

The above figure shows mechanistic diagram of the ethanol-induced mitochondrial dysfunction. Increased reactive oxygen species (ROS) generation by CYP2E1 and impaired electron transport chain (ETC) function are critical components with major player's superoxide ($O_2{\cdot}^-$), hydrogen peroxide (H_2O_2), and hydroxyl radicals ($HO{\cdot}$) causing lipid peroxidation and cellular injury.

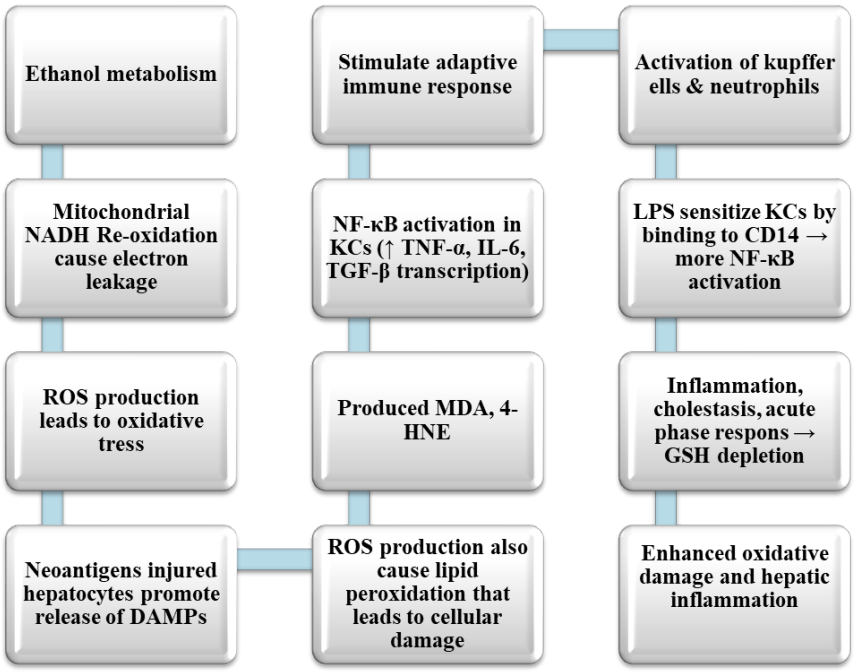

FIGURE 1.3: Ethanol metabolism elevates mitochondrial ROS, causing oxidative stress.

1.6 Cyclooxygenase-2 Pathway

NF-kB up regulates COX-2 and leads to the biosynthesis of prostaglandin E2 (PGE 2). This PGE 2 is a damaging amplifier and it can mobilize inflammatory cells and they can be activated to play a part in fibrosis and it will help sustain liver damages. COX-selective 2 inhibition interferes with biosynthesis of PGE 2 leading to inhibition of this harmful inflammatory-fibrotic cascade. More importantly, it does so without removing the protective roles of COX-1, like the preservation of integrity of gastric mucosa.Cyclooxygenase (COX) enzymes catalyze the rate-limiting step of the bioactive prostaglandins (PGs), formation from arachidonic acid (AA). COX-2 is responsible for the formation of the pro-inflammatory PG, prostaglandin E2 (PGE2), by oxidizing AA. PGE2 is then transported intracellular by the prostaglandin transporter (PGT) and signaling is initiated through the activation of EP2 and EP4 receptors leading to downstream cAMP signaling. This signaling pathway mediates inflammation, pain sensation, cell growth and tissue injury [37]. Selective inhibition of COX-2 represents a viable strategy to attenuate inflammation while minimizing gastrointestinal adverse effects commonly associated with non-selective NSAIDs.

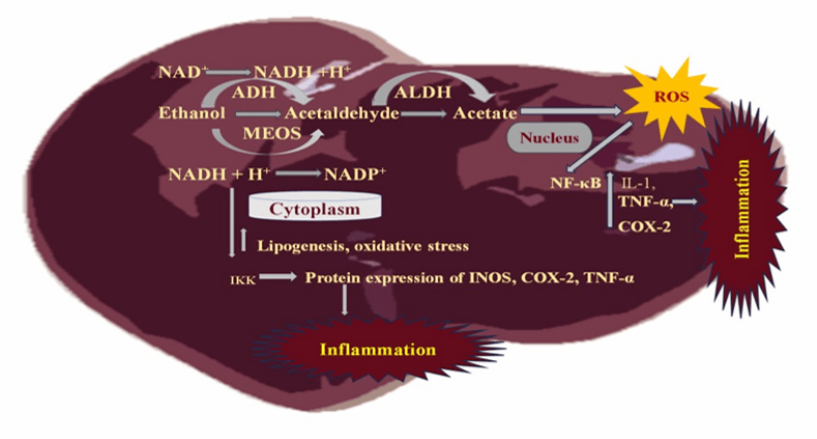

FIGURE 1.4: Ethanol metabolism and ROS production leads to inflammation.

The above figure shows illustrating ethanol metabolism leading to NF-κB activation, pro-inflammatory cytokine release (TNF-α, IL-6, COX-2). The figure emphasizes ROS-mediated Kupffer cell activation, DAMP release and recruitment of various immune cells to continue the chronic hepatic inflammatory response.

1.7 COX-2 as a Therapeutic Target

COX-2 induction by ethanol-derived ROS and NF-κB leads to excessive PGE_2, which recruits neutrophils, activates HSCs, and sustains cytokine release. Selective COX-2 inhibition (by etoricoxib) interrupts this loop without disrupting COX-1-mediated mucosal protection, offering a safer alternative to non-selective NSAIDs. Etoricoxib was chosen because it is highly selective to COX-2, has a long half-life and established the anti-inflammatory effect having little gastrointestinal side effects. This its capability of reducing NF-κB and TNF-α signaling further evidences its role as a hepatoprotective agent in disposal of injury incurred by the use of ethanol. Etoricoxib is a highly selective, second-generation, COX-2 inhibitor. It exert its anti-inflammatory, analgesic, and anti-fibrotic properties by blocking PGE2 synthesis and down regulating NF-κB-mediated cytokine expression [38]. Etoricoxib selective COX-2 inhibitor and ibuprofen as non-selective cyclooxygenase (COX-) inhibitor used as hepatoprotective agent, in mice model of ethanol induces hepatotoxicity. Etoricoxib, offers a promising pharmacological profile by targeting

inflammation while preserving COX-1-mediated protective functions. Its ability to reduce prostaglandin E2 synthesis suggests potential in curbing ethanol-induced inflammatory responses without eliciting significant off-target toxicity [39].

1.8 Therapeutic Role of Ibuprofen

Ibuprofen is non-selective COX-1 and COX-2 inhibitor. It inhibits prostaglandin production [40]. Ibuprofen is a traditional nonsteroidal anti-inflammatory drug commonly used for its analgesic, anti-inflammatory, and antipyretic properties. Ibuprofen used to relieve minor pain and inflammation, like headache, muscular aches, toothache, fever, backache, and dysmenorrhea. Ibuprofen has a wide therapeutic window, range for its analgesic, antipyretic, and anti-inflammatory effects ($\sim$10–50 mg/l) [40].

In this context, the present study was designed to evaluate the hepatoprotective potential of etoricoxib in a mice model of ethanol-induced hepatotoxicity. Biochemical markers ALT, AST, TNF-α, and histopathological observations were assessed. This research aimed to determine the extent to which etoricoxib can modulate oxidative stress and inflammatory pathways in ethanol-exposed liver tissue by inhibiting COX-2. The study seeks to provide a mechanistic foundation for the therapeutic use of COX-2 inhibitors in the prevention and management of ethanol-related liver disease, potentially paving the way for safer and more targeted interventions in hepatic inflammation.

Chapter 2

Literature Review

2.1 Introduction

This chapter aims to offer a thorough overview of the mechanisms responsible for alcohol-induced damage to the liver. Considering the oxidative stress, inflammatory mechanisms, and COX-2-linked mechanisms that lead to liver injury. Explaining the pathophysiological consequences of ethanol metabolism and pro-inflammatory mediators that promote hepatic damage. This involve the pharmacological armamentarium of etoricoxib and its potential usage as a therapeutic agent to prevent liver injury secondary to ethanol. Understanding these mechanisms will also help in providing a rational basis for the consideration of etoricoxib as hepatoprotective. Alcohol is the world's most widely abused psychomotor drug, and its excessive consumption is linked to numerous degenerative and inflammatory conditions affecting multiple organs, including the liver, brain, heart, kidneys, skeletal muscles, and pancreas. Ethanol is metabolized in the liver mainly by ADH, MEOS yielding more ROS and oxidative-stressed hepatic cells. The interrelationship between fatty acid oxidation and ethanol metabolism plays a major role in the development of hepatic steatosis and injury. In 80% of unselected heavy drinkers who consume an excess of 80g of alcohol a day have higher chances of AFLD. Cirrhosis results in 1.32 million deaths every year, making it the 11th leading cause of death worldwide [41].

Studies using gramicidin A-based fluorescence assays demonstrate that ethanol alters lipid bilayer properties, reducing membrane fluidity [42]. Evidence from Patel and his collegues study in 2022 suggests that chronic ethanol consumption affects gut microbiota, increases intestinal permeability and systemic inflammation. All of these changes in the gut microbiota and the associated inflammatory process, along with dysfunctional adipose tissue, abnormal secretion and lipid metabolism, drive increased liver injury in the ALD [43]. Recent research (Shukla *et al.*, 2021) has started to identify that chronic stress and elevated corticosterone levels increase alcohol-related gut–liver axis dysfunction due to disruptions of epithelial tight and adherens junctions, increased gut permeability, increased endotoxemia, increased systemic and hepatic inflammation, and increased neuroinflammatory responses [44]. By Yongke Lu and Joseph George study in the 2024, demonstrated the interrelationship between hepatic fatty acid oxidation and ethanol metabolism, impairs mitochondrial β-oxidation by generating excess NADH, altering cellular redox status, and inhibiting fatty acid oxidation regulatory enzymes. This metabolic dysregulation results in hepatic lipid accumulation and steatosis. Further, the loss of cellular energy homeostasis caused by ethanol metabolism encourages those fatty acids towards oxidative stress and liver injury. This study describes, findings that elucidate the multifactorial mechanisms by which chronic ethanol exposure induces hepatocellular injury, encompassing oxidative stress, mitochondrial dysfunction, impaired lipid metabolism, and systemic inflammation [45]. According to (Xu *et al.* in 2021), alcohol consumption worsens viral hepatitis B and C by stimulating viral replication, impairing immunity, and inducing oxidative stress, which hastens the liver fibrosis, cirrhosis, and hepatocellular carcinoma process [46].

In 2019 Ren *et al.*, study demonstrated that the liver injury and inflammation inhibit ethanol and acetaldehyde metabolism through the downregulation of key enzymes in the process of alcohol metabolism. This metabolic inhibition increased ethanol, acetaldehyde concentrations, and affected the behaviors in alcohol-drinking mice [47]. Ethanol directly interacts with proteins altering their biological functions, may be damaged mucous membranes, which disturbs the processes of intestinal absorption and increases the risk of developing esophageal cancer and gastritis [48]. The research conducted by Mackus *et al.*, in 2020 indicates that ethanol metabolism

at a faster rate is associated with milder hangovers, but in general, blood ethanol levels and acetaldehyde levels were not associated with greater hangover severity, while delayed oxidative stress and inflammation raised cytokines played a substantial role in hangover pathology [49]. A studies in 2010 established that chronic ethanol exposure causes mitochondrial dysfunction, chronic production of ROS, activation of NF-κB, and ultimately the release of pro-inflammatory mediators such as TNF-α, IL-1β, and IL-6 [50]. Previous studies have reported that ALD is caused by the metabolism of ethanol via ADH, CYP2E1, catalase, which causes oxidative stress and alters regulatory factors such as kinases, transcription factors, and miRNAs (Yan *et al.* In 2023). This causes mitochondrial stress, ER stress, inflammation, fibrosis, and gut-liver axis impairments [51]. Shen, H., *et al.*, in 2025, emphasize that targeting enzymes that metabolize ethanol, like ALDH2 and ADH, may be a useful new therapeutic option for alcohol use disorder (AUD). While disulfiram and genetic approaches are able to reduce alcohol consumption by inhibiting ALDH2, caution must exercised to avoid acetaldehyde accumulation and to evaluate the contribution of acetaldehyde to alcohol-related carcinogenesis [52].

In studies the pathophysiology of ethanol-induced hepatotoxicity, and repeatedly emphasized the relevance of oxidative stress, mitochondrial dysfunction, and inflammatory natures of the process, showed that ROS from ethanol metabolism directly activate HSCs and subsequently inflammatory processes, initiating fibrogenic processes. Research conducted by Contreras Zentella *et al.*, in 2022, reviewed the mechanisms of hepatic ethanol metabolism, that ADH, CYP2E1 (MEOS), and catalase pathways produce ROS, depleting antioxidant defenses such as glutathione. This imbalance promotes lipid peroxidation, mitochondrial dysfunction, inflammation, and steatosis, suggesting that therapeutic interventions should target both metabolic and antioxidant pathways [28]. Cho and his collegue in 2021, demonstrated that high dietary fructose triggers a CYP2E1-dependent increase in oxidative and nitrative stress, leading to nitration of intestinal tight and adherens junction proteins. This results in leaky gut, endotoxemia, hepatic inflammation and fibrosis, revealing a mechanistic link between fructose intake and liver disease exacerbation [53]. According to published findings of (Liu *et al.*, 2025) demonstrated that ethanol metabolism via ADH, CYP2E1, and catalase generates oxidative stress

contributing to AUD pathophysiology through genetic predisposition, inflammatory cascades, and neurodegeneration, highlighted ongoing clinical trials exploring antioxidant interventions combined with metabolic and genetic targets [54].

Previous studies showed the simultaneous loss of endogenous antioxidant defenses, increases in TNF-α and IL-1β in livers of mice. It has been demonstrated that more mechanistically, ethanol's inhibition of mitochondrial ATP production and electron transport leads to increased hepatocellular apoptosis (Thomes *et al.* in 2021) [55].

Together, they suggest ethanol's multi-faceted toxicity in the liver, reinforcing the need for more targeted anti-inflammatory and antioxidant treatments. In 2022, Shams and Eissa published a study, investigating the gastroprotective effects of quercetin against ethanol-induced gastric ulceration in rats. Their results showed that quercetin significantly improved the damage to the gastric mucosa by enhancing the antioxidant defense system by activating the Nrf2/HO-1 pathways, which are important in relieving oxidative stress.

In addition, quercetin inhibited important inflammatory pathways, including HMGB1 / TLR4 / NF-κB, which measurably reduced the pro-inflammatory cytokine TNF-α. Finally, quercetin inhibited apoptosis by manipulating the Bax/Bcl-2 ratio towards cell survival. Together these mechanisms explained the gastroprotective effects of quercetin and indicates the possibility of using quercetin as a therapeutic against ethanol-induced gastric injury [56].

In 2021 Raish and his collegue, demonstrated that sinapic acid significantly protects rats from ethanol induced gastric ulcers by activating the Nrf2/HO 1 antioxidant pathway, inhibiting NF κB–mediated inflammation, reducing oxidative stress and apoptosis, and improving mucosal integrity outcomes comparable to the standard drug omeprazole [57].

In 2012 Cederbaum, and Zakhari, demonstrates that excessive ethanol metabolism, particularly through the CYP2E1 pathway, generates ROS such as superoxide anions, hydrogen peroxide, and hydroxyl radicals. These reactive molecules impair cellular function by inducing lipid peroxidation, protein modification, and DNA

damage [58]. Study in 2021, reported ethanol metabolism refers to various pathways including oxidative (ADH, ALDH, CYP2E1/MEOS, catalase, AOX/XOR) and non-oxidative ROS with the gut microbiome also playing an essential role in ethanol clearance and progression of liver disease [59].

Recent studies have shown that hydroxyethyl radicals can alkylate liver proteins resulting in the production of specific antibodies that mediate immune toxic reactions in animal models [60]. Study involving C57BL/J mice demonstrated that chronic consumption of a high-fat diet containing ethanol significantly elevated hepatic iron levels, leading to increased oxidative damage [61].

Research indicates that, interplay between oxidative stress and inflammation leads to hepatocyte apoptosis and recruitment of immune cells that exacerbate tissue damage. This dual mechanism underscores the complexity of ALD [62].

Globally, alcohol-associated liver disease (ALD) leads to significant liver-related morbidity and mortality. About 80% of chronic heavy drinkers will develop steatosis, 10-35% will progress to alcoholic hepatitis, and about 10-15% will develop cirrhosis [63]. Malik and his collegue study in 2023, demonstrated that geraniol significantly decreased paw swelling, repaired joint integrity in a rat model of inflammatory arthritis, and had equal affinity to methotrexate.

Geraniol also normalized hematological and inflammatory markers TNF α, IL 1β, CRP, rheumatoid factor, expressed significantly lower COX 2, mPGES 1, PTGDS, and MMP 1 levels, demonstrating geraniol's anti-inflammatory and anti-collagenase effects [64].

Zakiyah and colleagues (2022) wrote a comprehensive review of selective COX-2 inhibitors (celecoxib, rofecoxib, etoricoxib), which indicated they can inhibit prostaglandin synthesis through the inhibition of COX-2 and modulating PD-L1/ PGE_2, MAPK/PI3K, STAT3, and growth factor pathways involved in inflammation, tumor immune response, and regulation of oxidative stress [65]. Etoricoxib role as a selective COX-2 inhibitor that reduces prostaglandin synthesis without significantly affecting COX-1 activity. Etoricoxib reduced inflammation, oxidative stress,

and collagen deposition significantly, indicating potential antifibrotic and hepatoprotective actions. It seemed to exert its effects by inhibiting the COX-2 receptor and regulating pro-inflammatory pathways in liver damage [66]. Etoricoxib hepatoprotective effects may be attributed to its modulation of oxidative stress markers and mitochondrial function. Recent evidence suggests that etoricoxib stabilizes mitochondrial membrane potential, thereby preventing cytochrome-c release and caspase-3 activation, key mediators of ethanol-induced apoptotic liver injury. The drug's ability to inhibit COX-2 also impedes the amplification loop of inflammation, in which prostaglandins stimulate further cytokine production and leukocyte infiltration [67]. Recent findings from large-scale clinical trials evaluating newer COX-2 inhibitors (coxibs), which used ibuprofen as an active comparator, corroborate previous research demonstrating that ibuprofen provides comparable therapeutic efficacy to both coxibs and conventional NSAIDs [68]. Ibuprofen is commonly used in the management of numerous inflammatory, musculoskeletal and rheumatic disorders, because they are highly effective having minimal toxicities [69].

Umoh *et al.* Study in 2022 evaluated the hepatotoxicity of NSAIDs (piroxicam, diclofenac, ibuprofen) applied separately and in combinations in Wistar rats. While there was only a negligible impairment in the biochemically insensitive liver parameters (ALT, AST, bilirubin), histological assessment illustrated congestion of the portal vein, hepatic bile ducts filled with blood, distortion of the sinusoidal architecture, and degeneration of the hepatocytes, suggesting that either high-dose NSAID exposure or the combination of NSAIDs can impact liver architecture, despite negligible impairment in standard enzyme assays [70]. Recent resreach showed low-dose anethole and ibuprofen in rat model reduced inflammation well, by decreased paw edema, synovial leukocyte infiltration, partially protected against hepatic metabolic alterations seen with arthritis and NSAID use. This is valuable because combine plant-derived anti-inflammatory agents, such as anethole, with NSAIDs to achieve better efficacy, with less chance for hepatic side effects [71]. According to (Varrassi et al 2020), ibuprofen retains a favorable safety profile among the NSAIDs, with relatively low gastrointestinal and cardiovascular risks at clinically relevant doses. There are still risks for adverse effects due to renal and hepatic temporary and permanent adverse effects, and risk of infection adverse effects that depend

on the dose, on patient characteristics and medications at the same time. Growing evidence suggested endocrine-disrupting properties of ibuprofen and possible anticancer properties of ibuprofen, which emphasizes that ibuprofen is relatively safe, but its risk profile is still unique among the NSAID classes [72]. Pharmacogenomics research on ibuprofen has explored how genetic polymorphisms influence its pharmacokinetics, pharmacodynamics, safety, and therapeutic efficacy [73]. Additionally, a 2020 comparative study suggested that etoricoxib may be more effective than ibuprofen for pain management [74].

2.2 Aims and Objectives

The study aimed to evaluating the role of etoricoxib in attenuating inflammation in ethanol-induced Hepatotoxicity. The main objectives of this study were to assess the biochemical changes associated with ethanol-induced hepatotoxicity by measuring the serum levels of liver-specific enzymes, alanine aminotransferase (ALT) and aspartate aminotransferase (AST), by using an approved commercially available standardized diagnostics kits. To assess the inflammatory response, the second objective was to measure the level of the pro-inflammatory cytokine TNF-α by using enzyme-linked immunosorbent assay (ELISA), which helped to understand TNF-α role in ethanol-induced liver injury. Finally, how heptoprotective and anti-inflammatory properties of etoricoxib as a selective COX-2 inhibitor was experimentally established by measuring the TNF-α expression. If the levels of liver enzymes and TNF-α decrease in the ethanol-treated mice, we could conclude that etoricoxib was effective in reducing inflammation of the liver caused by ethanol exposure, and we could support the role of etoricoxib in providing protective effects on the liver.

Chapter 3

Materials and Methods

3.1 Introduction

This chapter provides an overview of experimental studies design, methodology, animal model, dosing strategy, analytical methods, and ethical considerations that guided the investigation of the anti-inflammatory effects of etoricoxib with ibuprofen as a comparator in ethanol-induced hepatotoxicity. The study has been deliberately organized to reflect the underlying pathological mechanisms involved in ethanol liver injury. A systematic approach was undertaken to maximize scientific validity, objectivity, repeatability, and translational relevance. Ethanol-induced hepatotoxicity was induced using repeated intraperitoneal injections of absolute ethanol to reflect repeated exposure to chronic ethanol and replicate the critical clinical features associated with alcoholic liver disease (ALD) including hepatic neuronal inflammation, increased hepatic enzymes and liver tissue necrosis. The adult Balb/C mice used for the studies were chosen for their relatively stable genetic make-up, specific physiological responses to toxic substances and non-individualized characterizations assessing their use as a model for hepatotoxicity.

To evaluate the possible hepatoprotective and anti-inflammatory efficacy of etoricoxib a selective inhibitor of COX-2 and ibuprofen a nonselective NSAID, complete dosing protocols were utilized in an ethanol-fed hepatotoxicity model.

As parameters of liver injury serum ALT and AST were biochemically determined. Inflammation was measured using TNF-α via ELISA, and total protein content from all serum samples determined using Bicinchoninic Acid (BCA) protein assay, for systemic effects monitoring.

Histopathology of liver samples were generated using hematoxylin and eosin (H&E) stained liver tissue samples to assess morphological alterations, cellular infiltrations, and necrotic lesions. The use of these separate *in vivo*, biochemical, and histological assessments provided baseline understanding of the liver injury from each ethanol dose and degree of hepatoprotection provided by each test drug.

As part of the *in vivo* studies, we used molecular docking studies to predict the binding affinity and interaction of etoricoxib and ibuprofen as ligands towards important molecular targets involved in hepatic inflammation COX-2, TNF-α, and NF-κB. We used tools such as AutoDock, PyMOL, and Discovery Studio to simulate ligand-protein interactions, to get the different binding conformations, and to get binding energy. The in-silico data provided the mechanism of action to which the anti-inflammatory effect observed *in vivo* could be associated.

The approaches outlined in this chapter provide a framework to evaluate both the biochemical and molecular pharmacological action of etoricoxib on ethanol-induced liver injury. All methods outlined in this chapter adhered to internationally accepted ethical principles as well as institutional animal care guidelines.

The image 3.1 shows the various steps used in the *in vivo* research experiment. Figure 3.1 show experimental study were start from randomly assigning mice into groups, marking, and acclimatizing mice, followed by recording body weight and dosing.

On dissection day, blood was collected via cardiac puncture, midline laparotomy was performed, and liver was extracted. The liver collected was used for, for BCA protein assay, ELISA for TNF-α, determination and performed H&E staining for histological or biochemical changes. (Photograph taken at faculty of Pharmacy, Capital University of Science and Technology).

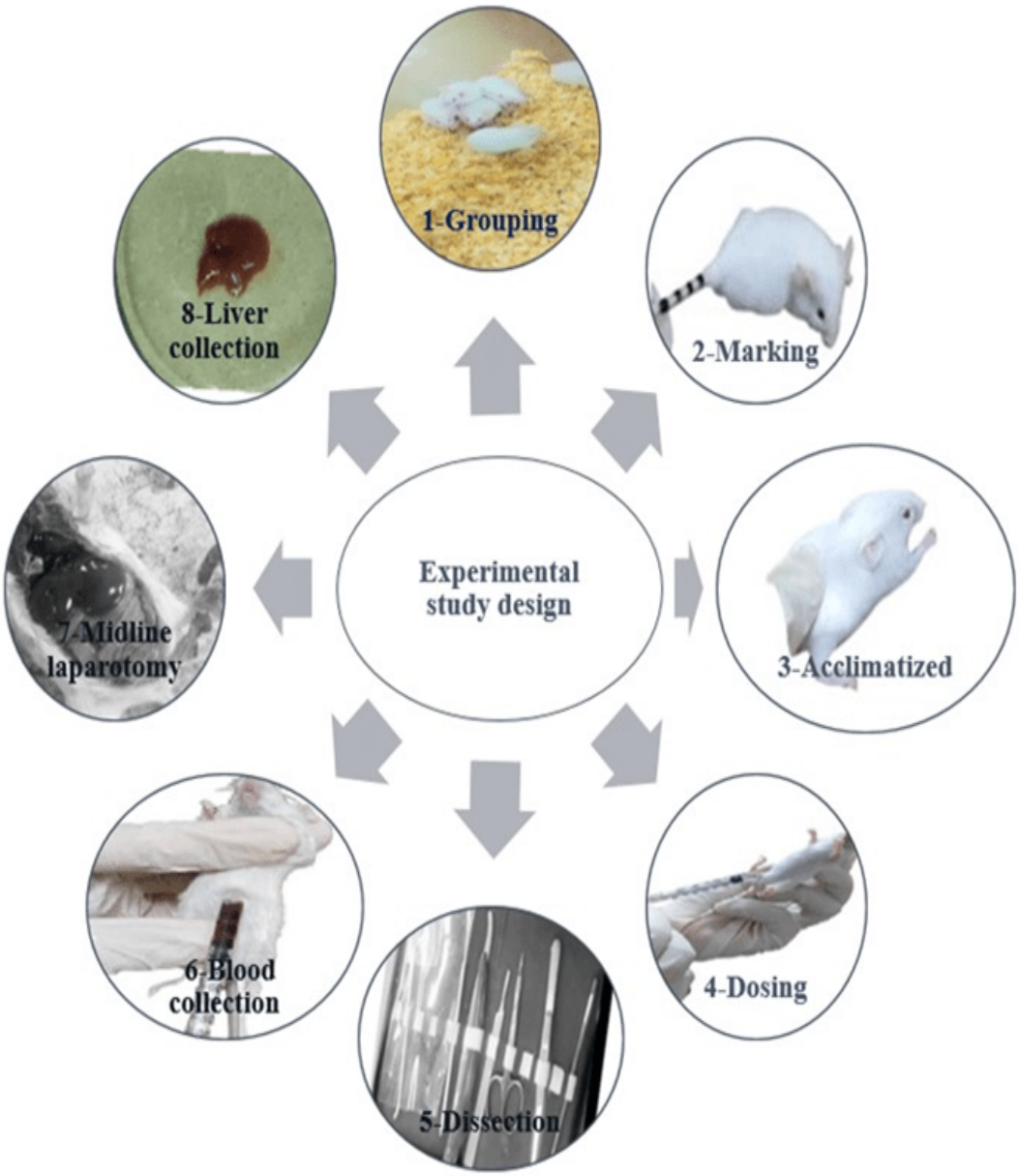

FIGURE 3.1: Experimental study design representing the *in vivo* study protocol in Ethanol-Induced Hepatotoxicity.

3.2 Ethical Statement

All experiments procedure involving animals were performed to comply with national regulations and institutional policies for the ethical care and use of laboratory animals. The study protocol (REC/Fop/F2024/16) was reviewed and approved by the Research and Ethical Committee (REC) of the Capital University of Science and Technology, Islamabad.

3.3 Experimental Animal

Thirty healthy Balb C mice (4 weeks old weighing 25g-30g) were purchased from the in-house breeding facility of Capital University of Science and Technology, Islamabad. Mice were housed under a controlled environment (22 ± 2°C, relative humidity 55 ± 5%) and 12 h light/dark cycle with ad libitum access to food and water. Mice were acclimatized to laboratory conditions for one week prior to experimentation [75].

3.3.1 Food Composition

Mice used in research were typically fed a balanced pellet diet designed to meet their nutritional needs. This diet usually contains about 18-24% protein, 4-6% fat, and 40-60% carbohydrates, along with fiber, vitamins, and essential minerals as shown in table 3.1. These ingredients often included fish, flour, bran and powdered milk. Consistent and standardized diets ensured mice health and reliable experimental results.

TABLE 3.1: Composition of animal food

Food item	**Quantity (5.0 kg)**	**Quantity (10.0 kg)**
Fish	750 g	1. 5 Kg
Wheat Flour	3.25 Kg	6.5 Kg
Vitamins/Minerals	75 g	150 g
Dry Skimmed Milk	200 g	400 g
Chokar	750 g	1. 5 Kg

3.3.2 Mice Bedding

Mice were housed on bedding materials that provide comfort, absorb moisture, and reduce odor. Common bedding types include wood shavings (such as aspen) were used. The choice of bedding should be important as it can influence animal health, behavior, and experimental outcomes. Bedding was changed on a daily basis to provide them with a non-toxic, dust free and stress-free environment for the mice.

3.3.3 Animal Handling

Mice were restrained using standardized tail and scruff handling techniques to minimize stress. Each animal was placed on the surface of a wire cage lid. The tail was held at its base with the thumb and forefinger of one hand, while the other hand was positioned on the lower back.

Gentle pressure was applied in a forward direction towards the loose skin at the back of the neck, ensuring closure around the ears. The scruff was then firmly grasped, and the tail was drawn towards the wrist, with the little finger securing the tail in place.

The grip was maintained firmly enough to prevent struggling while remaining gentle to allow normal respiration [76].

FIGURE 3.2: Animal handling using standardized tail and scruff handling techniques to minimize stress.

Figure, demonstrating appropriate techniques for restraining mice in order to minimize stress to the animals during procedures.

The tail and scruff handling method was used to provide secure immobilization during injection (Photograph taken at faculty of Pharmacy, Capital University of Science and Technology).

3.4 Grouping and Experimental Design

FIGURE 3.3: Mice were acclimatized to animal facility conditions prior to the commencement of experimental study.

This figure shows, gentle handling method to minimize stress and ensure the mice's comfort during routine experimental procedures, in accordance with ethical animal care practices. (Photograph taken at faculty of Pharmacy, Capital University of Science and Technology).

Animals were randomly assigned into experimental groups using a simple randomization method to reduce bias. Mice were identified by cage labeling and non-invasive marking techniques such as tail marking. A tail-marking technique was employed to ensure consistent individual identification of animals throughout the study. This method involved marking the tails with unique combinations of transverse lines and circles of varying sizes. Mice were marked prior to the experimental treatment with the identifiers.

Mice-1 had one small circle across the tail, mice-2 had two small circles on the tail that were slightly separated, mice -3 had three small circles evenly spaced across the tail, mice-4 had four small circles on the tail, mice-5 had one large circle on the tail that was clearly distinguishable from the small circles on the previous animals, mice-6 had two (small and large) circles, separated by a small gap; the first of the circles had a large cross-sectional area and the second circle had a small area, mice-7 had three circles on the tail with the first a large circle and the second and third

having small size, mice-8 had four circles; one large circle at one end and three smaller circles spaced out appropriately. This pattern continued for the subsequent animals allowing for accurate and non-invasive identification throughout the study period.

FIGURE 3.4: Mice identification and marking protocol for experimental studies.

The image depicts typical temporary tail marking methods for identifying individual lab mice, during short term experiments. (Photograph taken at faculty of Pharmacy, Capital University of Science and Technology).

3.4.1 Grouping of Mice

30 healthy Balb/C mice (weighing 26-30 g) were randomly allocated into five experimental groups (n = 6). Animals were marked individually and allocated into groups in a blinded manner to eliminate selection bias. All mice received their respective treatments via the intraperitoneal (i.p.) route once daily for nine consecutive days. Ethanol was used to induce hepatotoxicity, and the therapeutic agents (etoricoxib and ibuprofen) were administered. Experimental groups and treatments description shown in table 3.2.

FIGURE 3.5: Randomization strategy for experimental grouping of mice (n = 6 per group).

Mice were randomized into distinct treatment groups, with 6 animals per group to ensure uniform distribution and minimize bias.

One group of mice (n = 6) was housed per cage, representing a distinct experimental group (e.g., control, ethanol, treatment), and mice were assigned using randomized control method. (Photograph taken at faculty of Pharmacy, Capital University of Science and Technology).

TABLE 3.2: Experimental groups and treatments description

Group	**Treatment Description**
Group-1 (Control)	Received an equivalent volume of 1% DMSO in saline (i.p.) and served as the control group.
Group-2 (Ethanol-only)	Received ethanol at a dose of 20% v/v (5g/kg) (i.p.) once daily for nine consecutive days to induce hepatotoxicity.
Group-3 (Etoricoxib Low Dose)	Administered etoricoxib at a dose of 25 mg/kg (i.p.), 30 minutes after ethanol 20% v/v (5g/kg) (i.p.) administration.
Group-4 (Etoricoxib High Dose)	Administered etoricoxib at a dose of 50 mg/kg (i.p.), 30 minutes after ethanol 20% v/v (5g/kg) (i.p.) administration.
Group-5 (Ibuprofen)	Received ibuprofen at a dose of 50 mg/kg (i.p.), 30 minutes after ethanol 20% v/v (5g/kg) (i.p.) administration.

3.5 Routes of Administration

The route of administration significantly influences the pharmacokinetics, pharmacodynamics, and toxicity of pharmacological agents. In laboratory animals, the primary routes include intravenous (IV), subcutaneous (SC), intraperitoneal (I.P.), and oral administration. In this study, I.P route was used for drug delivery in a mice model of ethanol-induced hepatotoxicity.

3.5.1 Intraperitoneal Route of Drug Administration

The I.P. route is quick and minimally stressful for animals. It involves holding the mice in a supine position with its head tilted lower than the posterior part of the body and insertion of the needle in the lower quadrant of the abdomen (at $\sim 10^o$ angle) with care to avoid accidental penetration of the viscera [78]. A 1-ml insulin syringe fitted with a 30-gauge needle was used to deliver all medications. In order to reduce the possibility of puncturing internal organs, the lower right abdominal quadrant was chosen for injection. To lessen stress during administration, mice were gently restrained using common tail and scruff handling techniques.

FIGURE 3.6: I.P. Injection in the lower right abdominal quadrant of mice.

I.P. injection site (lower right quadrant) to avoid injuring visceral organs puncture. The needle was inserted at a 10^o angle; if the animal is properly restrained, accurate dosing should occur with minimal discomfort. (Photograph taken at faculty of Pharmacy, Capital University of Science and Technology).

3.6 Chemicals

All the reagents used for the experiments were of standard analytical grade. Ethanol (20%v/v) was used to induce hepatotoxicity, was procured from the Faculty of Pharmacy CUST.

Etoricoxib and ibuprofen were generously provided by Jupiter Pharma, Rawat, Islamabad. Etoricoxib was evaluated for its potential hepatoprotective and anti-inflammatory effects, while Ibuprofen served as a standard reference drug.

3.6.1 Drug Solubility

The test compound was initially mixed with normal saline and vortexed due to the limited water solubility. However, it was not dissolved entirely. To get better solubility, a co-solvent method was utilized, 40 μL of dimethyl sulfoxide (DMSO) was added to the compound and vortexed until dissolved.

After all the drug was dissolved, 960 μL of normal saline was added, and solution was mixed very thoroughly. The 40 μL DMSO/960 μL normal saline provided a final homogenous solution of 1 mL that was ready for intraperitoneal injection. List of equipments shown in table 3.3.

Table 3.3: List of equipments

Sr.no	**Equipment**
1.	Analytical weighing balances
2.	Micro-centrifuge tubes (Eppendorf)
3.	Micropipette
4.	vortex mixers

3.6.2 Drug Preparation

Formula for Dose Calculation

Dose = Body weight (g) * Dose (mg/kg)/1000

Volume Required (mL) = (Required Dose (mg)/Stock Concentration (mg/mL)

3.6.2.1 Dose Calculations for Ethanol 20% v/v (5g/kg)

Ethanol Dose 20% v/v (5 g/kg)

for 30 gram mice: Ethanol Density: 0.789 g/mL

Target Dose: (5 g/kg) body weight

Required Ethanol (g)=30 g×(5 g/kg)1000 = 0.15g

Volume (mL)=0.789 g/mL 0.15 g = 0.19 mL.

3.6.2.2 Dose Calculations Etoricoxib (25 mg/kg), Etoricoxib (50mg / kg), (Ibuprofen 50mg/kg)

For the preparation of a 25 mg/kg etoricoxib solution (1 mL), 2.5 mg of etoricoxib was accurately weighed and initially dissolved in 40 μL of DMSO in a sterile eppendorf tube. Subsequently, 960 μL of normal saline was added to achieve a final volume of 1 mL. The solution was vortexed thoroughly to ensure complete dissolution. The drug was fully soluble in DMSO prior to dilution. For a 30g mice, the required dose was 0.75 mg, and the volume administered was 0.3 mL of the prepared stock solution. For the preparation of a (50 mg/kg) etoricoxib solution (1 mL), 5 mg of etoricoxib was accurately weighed and dissolved in 40 μL of DMSO, followed by the addition of 960 μL of normal saline. The solution was vortexed to obtain a homogeneous and clear solution. For a 30g mice, the required dose was 1.5 mg, and the volume administered was 0.3 mL of the stock solution. For the preparation of a (50 mg/kg) ibuprofen solution (1 ml), 5 mg of ibuprofen was accurately weighed

and dissolved in 40 μL of DMSO. Then, 960 μL of normal saline was added and mixture was vortexed thoroughly. A clear and uniform solution was obtained. For a 30g mice, the required dose was 1.5 mg, and the injected volume was 0.3 ml.

3.6.3 Dosing Protocol

All drug administrations were performed by using insulin syringe 1ml, 30 gauge of BD Ultra-fine II needle to ensure precision of dose administration and minimal tissue trauma. All drugs were freshly prepared on the day of administration. Dose were calculated based on the individual body weight of each mice, which was recorded daily prior to dosing. This ensured accurate and consistent dose delivery across the study period. Ethanol 20% v/v (5 g/kg) was administered to induced hepatotoxicity. Mice received drug etoricoxib or ibuprofen 30 minutes' post-ethanol administration, to evaluate post-exposure hepatoprotective efficacy.

FIGURE 3.7: Daily body weight measurement of mice.

The figure illustrates the procedure for recording the body weight of each mouse daily using a digital balance. Regular weight monitoring was conducted to assess general health status, detect any adverse effects of treatments, and adjust dosing volumes accordingly during the experimental period. (Photograph taken at faculty of Pharmacy, Capital University of Science and Technology).

Lethargy, irritability, and weight loss were observed as symptoms of toxicity, especially following the third day of ethanol administration. After dosing for nine consecutive days, mice were anesthetized with chloroform and sacrificed on day ten via AVMA guideline. Blood was collected via cardiac puncture under deep anesthesia. Liver tissues were immediately harvested, rinsed in 0.9% saline and stored at -80^{o}C for biochemical analysis. Daily treatment schedule and observations for all experimental groups shown in table 3.4.

TABLE 3.4: Daily treatment schedule and observations for all experimental groups

Groups	**Dose administration (1-9 day)**	**Route**	**Monitoring**	**Observation**
Control group	1% DMSO in saline	i.p.	Record body weight. Monitor behavior.	Normal behavior, stable body weight
Ethanol group	Ethanol (5 g/kg) (20% v/v)	i.p.	Record body weight. Monitor behavior	↓Body weight, irritability post Day 3
Ethanol + Etoricoxib (Low Dose)	Ethanol (5 g/kg) + Etoricoxib (25 mg/kg)	i.p.	Record body weight. Monitor behavior	Mild protection, stable behavior
Ethanol + Etoricoxib (high Dose)	Ethanol (5 g/kg) + Etoricoxib (50 mg/kg)	i.p.	Record body weight. Monitor behavior	Improved clinical signs, more weight retention
Ethanol+ Ibuprofen (standard reference drug)	Ethanol (5 g/kg) + Ibuprofen (50 mg/kg)	i.p	Record body weight. Monitor behavior	Moderate protection, normal behaviour

3.7 Personal Protective Equipment and Biosafety Measures

All sample collection procedures were conducted using appropriate personal protective equipment (PPEs) in accordance with institutional biosafety protocols to minimize exposure to biological materials. All other PPEs as required by protocol/facility. Hands should be washed. Gloves changed during dose administration of different mice groups. Promptly dispose of used-sharps in the provided leak-proof, puncture resistant sharps container [79]. List of PPEs shown in table 3.5.

Table 3.5: List of PPEs

Sr.no	Item	Purpose
1.	Lab coat	To protect personal clothing and skin
2.	Gloves	To prevent contact with blood and tissues
3.	Eye protection	To shield against accidental splashes
4.	Surgical Mask	To reduce contamination and exposure risk

3.8 Euthanasia and Methods of Euthanasia

Euthanasia procedures were performed in compliance with the AVMA Guidelines for the euthanasia of animals (2020) and approved by the institutional animal care and use committee (IACUC). The word euthanasia means an easy death and should be regarded as an act of humane killing with the minimum of pain, fear and distress.

The procedure choice should approach as closely as possible the following criteria; it should be painless, produces rapid loss of consciousness and death, Interrupts consciousness and reflexes simultaneously, requires minimum restraint, avoids excitement and causes minimal psychological stress to the animals, appropriate for the age of the animal [80].

3.8.1 Methods of Euthanasia Fall into Categories Physical Method and Chemical Method

There are various physical method and chemical methods of euthanasia [81].

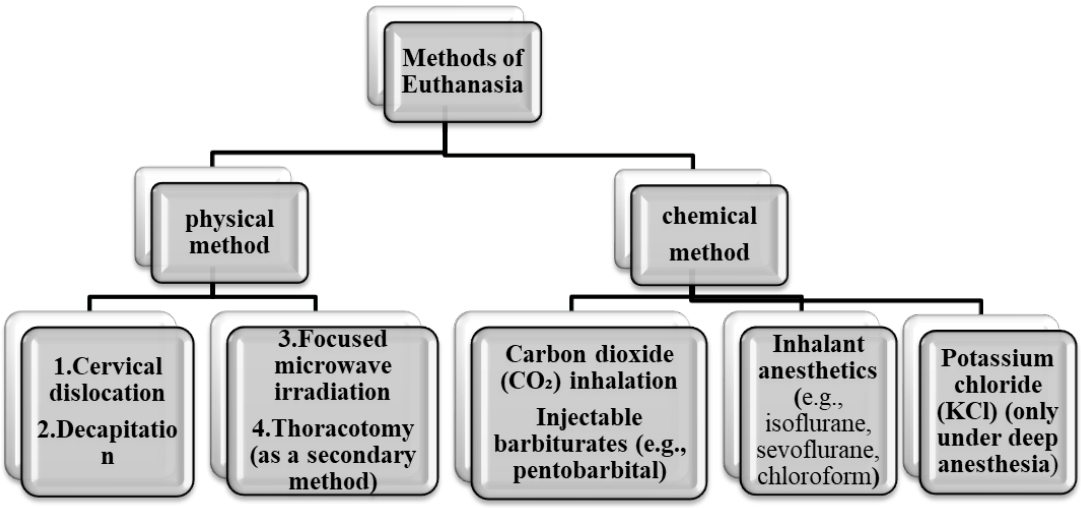

FIGURE 3.8: Classification of euthanasia techniques.

The above figure shows two primary classes of euthanasia, physical and chemical methods. In the case of physical methods, techniques that will rapidly lose consciousness mechanically (e.g., cervical dislocation, decapitation). The chemical method will use pharmacological agents that provide painless and humane death (inhalant anesthetics, Chloroform, barbiturates).

3.8.1.1 Chemical Method

The chemical inhalation method with chloroform was used in mice model of ethanol induced hepatotoxicity. Chloroform was chosen out of the various physical and chemical euthanasia techniques available for laboratory animals, for its ability to quickly induce unconsciousness, low handling stress, and compatibility with subsequent tissue analysis. Two to three milliliters of chloroform absorbed on cotton were used to pre-saturate an airtight desiccator before adding chloroform vapor. Individual mice were exposed to the fumes for two to three minutes until their corneal reflex and respiration completely stopped. The absence of cardiac activity was used

to confirm death, and a cardiac puncture was performed right away to obtain a sample [82]. Chloroform is a colorless, volatile liquid that is not very soluble in water. It has a pleasant, non-irritating odor. The chemical formula for chloroform is CHCl3, a molecular weight of 119.38 g/mol. Chloroform is a commonly used chemical in biological laboratories and for industrial processes [83]. Chloroform sedation has been used to sacrifice animals with apparently no undesirable effects. Animals were introduced into a desiccator containing their corresponding chemical. Prior to exposure, the chemical was soaked in cotton wool and placed in the desiccator for 2minutes to ensure circulation [84].

3.9 Blood Withdrawal Techniques

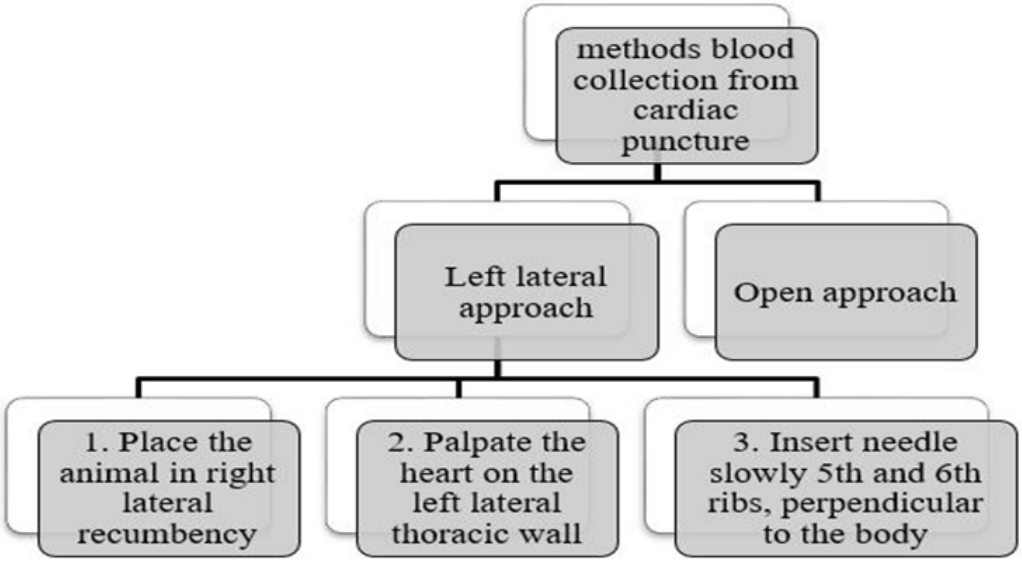

FIGURE 3.9: Blood withdrawal techniques in mice.

The figure shows comparative demonstration of multiple blood collection routes in mice, with a focus on the effectiveness of cardiac puncture for terminal serum.

Collection through tail vein, saphenous vein, and retro-orbital bleeding is appropriate for obtaining relatively small amounts of blood, but cardiac puncture, either under deep anesthesia or post-euthanasia, produces the maximum volume of blood collected (1.0-1.5 mL) with little hemolysis.

TABLE 3.6: Material required for blood collection

Sr.no	**Item**
1.	Chloroform
2.	Cotton
3.	Syringes
4.	Tubes for blood collection
5.	Gloves
6.	Mask

3.9.1 Cardiac Puncture

For terminal blood collection, animals were anesthetized deeply with chloroform. Once unresponsive, the animal was placed in dorsal recumbency [85]. Blood was collected by terminal cardiac puncture using a 1 mL sterile syringe with a 23G needle. The needle was inserted through the thoracic wall into the left ventricle at a 30-45^o angle, slightly left of the sternum and directed cranially. Upon entry, gentle aspiration was performed to draw 1.0-1.5 mL of blood. Collected blood was transferred to clean, labeled micro tubes [86]. Cardiac puncture method was selected for blood collection in mice model of ethanol-induced hepatotoxicity.

FIGURE 3.10: Blood withdrawal by cardiac puncture.

Terminal blood collection via cardiac puncture under deep anesthesia. The needle is advanced into the left ventricle at a 30-45^o angle, and blood is aspirated into sterile syringes for biochemical analysis. (Photograph taken at faculty of Pharmacy, Capital University of Science and Technology).

3.9.2 Blood Withdrawal By Cardiac Puncture Procedure

Deeply anesthetize the mice with the chloroform anesthetic agent prior to sample collection procedures. Place the animal in dorsal recumbency once the animal has reached an appropriate plane of anesthesia. Attached appropriate sized needle to a syringe and insert bevel up at a 30-40^o angle through the diaphragm, with syringe parallel to the midline of the mice. Insert needle slightly left under the sternum, directed toward the mice heart. The needle can be angled slightly towards the left shoulder. Retract the plunger slightly to create a vacuum inside the syringe and gently advance needle until blood flash appears in needle hub. Immobilize the needle and continue to aspirate until a sufficient amount of blood has been collected [87].

FIGURE 3.11: Tubes used for blood collection from mice.

The figure shows the microcentrifuge tubes used for collecting and storing blood samples obtained via cardiac puncture from mice. Collected samples were either processed immediately for serum separation enzymes analysis. (Photograph taken at faculty of Pharmacy, Capital University of Science and Technology).

3.10 Dissection and Liver Preservation

After cardiac puncture and euthanasia, a midline laparotomy was performed to access and extract the liver for further analysis [88].

3.10.1 Extraction of Liver

After cardiac puncture and euthanasia, a midline laparotomy was performed. The abdominal cavity was accessed via midline laparotomy. The skin and cutis were incised to a depth of about 2 cm with 11.5 cm surgical scissors. The connective tissue over the peritoneum was bluntly dissected with the tips of the scissors by gently spreading it to minimize trauma to the tissues. The peritoneum was then incised longitudinally along the Linea Alba to access the peritoneal cavity. The peritoneal cavity was expanded to improve visualization and access into the intra-abdominal organs using a holding suture through the xiphoid process area of the sternum. The holding suture was lifted and securely attached to the top of a Fluovac mask to create tension and tensioned to fully expand the operative field. A Calibri retractor was inserted into the peritoneal cavity to retract the surrounding tissues and keep the area exposed. Then abdominal cavity was elevated gently using the retraction forceps to expose the ventral surface of the liver, which was adhered to the diaphragm. As the liver was mobilized and elevated, the hepatic hilum was exposed. This was accomplished by retracting and mobilizing the gastrointestinal tract caudally to expose the bile duct. All fibrous connective tissue attaching the liver to its surrounding structures was carefully dissected and released until the liver was completely mobilized for resection. Following resection of the liver, the peritoneal cavity was provided sterile 0.9% sodium chloride (NaCl) lavage to wash out blood and debris. All abdominal organs were replaced in their original radiographic locations. The resected liver was washed immediately using 0.9% NaCl to remove blood and contamination from the surface of the liver. All liver related tissues were fixed in 10% phosphate buffered formalin (pH 7.4) for the preservation of tissue morphology prior to histopathology. Finally, fixed samples were stored at -4^{o}C for future biochemical and histological studies [89].

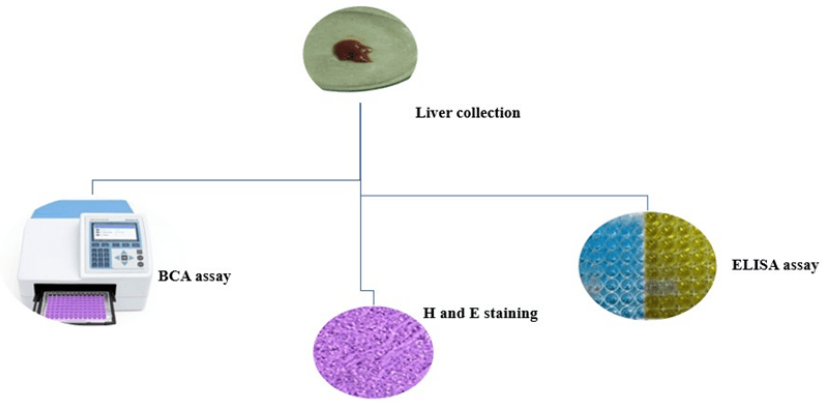

FIGURE 3.12: Liver collection and biochemical analysis.

Figure 3.12 illustrating the process of liver collection, which is followed by three distinct analytical techniques: BCA assay, H and E staining, and ELISA assay. The BCA assay is used to measure protein concentration, while H and E staining is employed to visualize tissue morphology. The ELISA assay, on the other hand, is utilized to detect and quantify specific antibodies or antigens. (Photograph taken at faculty of Pharmacy, Capital University of Science and Technology).

3.11 Biochemical Analysis

Biochemical analysis was conducted to evaluate hepatic injury and inflammatory response in the treated groups. The levels of ALT and AST in serum were measured in blood using commercial diagnostic kits. Liver homogenates were prepared for total protein quantification via the BCA assay and level of TNF-quantification via ELISA assay.

3.11.1 Liver Homogenate Preparation

Liver specimens were washed with ice-cold phosphate-buffered saline (PBS, pH 7.4) and transferred into pre-weighed eppendorf tubes. Based on sample weight (50-100 mg), an appropriate volume of 0.1% Tween 80 in PBS (pH 7.4) was added to each sample (e.g., for 50 mg tissue, 166.67 μL buffer was used). The samples were

homogenized using a tissue homogenizer (D160, China) [90]. Homogenates were centrifuged by using H-speed micro centrifuge SCI-24 at 8500 rpm for 30 minutes at 24^{o}C, and the supernatant was collected for BCA assay and ELISA assay.

3.11.1.1 Preparation of 0.1% Tween 80 PBS buffer 7.4

TABLE 3.7: Chemicals required for PBS buffer 7.4

Sr.no	Chemicals
1.	Tween 80
2.	1X PBS (Phosphate Buffered Saline), pH 7.4
3.	Measuring cylinder
4.	Pipette
5.	Stirring rod or magnetic stirrer

Preparation of Tween 80-PBS solution, take 0.1 ml (100μL) of the Tween 80 and add it to an appropriate amount of PBS. Stir the solution enough to ensure Tween 80 is completely dissolved and evenly distributed within the buffer. A magnetic stirrer was used to ensure consistent mixing. When the solution is clear and homogeneous, be sure to label the container with the name, concentration, and a date that indicates when it was prepared. The resulting solution can be stored at room temperature or tightly sealed in the fridge at 4^{o}C [91].

3.11.2 BCA Protein Assay Protocol

The Bicinchoninic Acid (BCA) assay is a widely used colorimetric method for quantifying total protein concentration in a sample. BCA protein assay kit Cat. No. P0012S was used by follow manufacturer's protocols. Purpose: To determine the protein concentration in liver tissue supernatant, using BCA assay.

TABLE 3.8: Materials required for BCA assay

Sr.no	Material
1.	Supernatant from liver tissue
2.	Append-draft tube

Table 3.8 continued from previous page

Sr.no	Material
3.	Homogenizer
4.	H- speed micro-Centrifuge
5.	Pipette
6.	BCA Protein Assay Kit (Reagent A and Reagent B)
7.	BSA Standard (2 mg/mL stock)
8.	96-well microplate
9.	Micropipettes and sterile tips
10.	Distilled water
11.	Plate reader

3.11.2.1 Liver Tissue Collection and Preparation

Liver tissues were carefully collected and weighed of the tissue was recorded, before being transferred directly to eppendorf tubes that were previously labeled and pre-weighed. The volume of 0.1% Tween 80 in PBS, pH 7.4 was added to each tube in correlation to the weight of the tissue.

The samples of all liver tissues were 50 mg to 100 mg in weight. Therefore, the proportion of the weight of the sample, 0.1% Tween 80 in PBS buffer (pH 7.4), in each tube was calculated. For example, if the sample of the tissue was 50 mg, which was approximately 166.67 μL was added to the tube, and this method was used for all samples with the same 0.1% Tween 80 in PBS (pH 7.4) solution. Homogenize the tissue thoroughly using a homogenizer. Centrifuge the homogenate at 8500 rpm for 30 minutes at 24^{o}C to remove tissue debris. Supernant was collected.

Preparation of Standards In 96-well plate standard serial dilutions from BSA stock (2mg/mL) were prepared. Use 20 μL of each dilution per well for the standard curve. Serial dilution (20ul, 15ul,10ul,7ul, 5ul, 2.5ul, 0.00). To make 20ul per well, distill water was added.

a) Sample preparation A sample Supernant was taken for the sample preparation with 1:10. Mix 1 of part sample with 9 parts distilled water (1:10 dilution).

b) Preparation of working reagent (WR) Reagent A and Reagent B are working reagent and were used as 50:1. If reagent A 50ul then reagent B will be 1ul. Freshly prepared before using. Add 200 μL of the WR to each well. Gently tap the plate to mixed for 30 second.

c) Incubation After adding the WR to samples and standards, incubated the plate at 37^{o}C for 30 minutes. Following incubation, plate was cool to room temperature (approximately 5-10 minutes) before proceeding.

d) Plate reader Measured absorbance at 562nm using a plate reader. Constructed the Standard curve and calculated sample protein concentrations based on absorbance values.

FIGURE 3.13: Use of a microplate reader to analyze BCA protein assay.

Figure 3.13 shows BCA assay based on the colorimetric detection of protein concentration. The protein reduces Cu^{2+} to Cu^{+} in an alkaline medium, bicarbonic acid chelates the Cu^{+}, resulting in color formation to produce a purple complex. The resulting colour can then be measured using the microplate reader at 562 nm. (Photograph taken at faculty of Pharmacy, Capital University of Science and Technology).

3.11.3 ELISA Test

Quantification of TNF-α level in liver homogenates was performed using a commercially available sandwich ELISA kit REF NO. PRS-2050Mo, LOT No 202312 in strict adherence to the manufacturer's protocol.

3.11.3.1 Assay Procedure

Dilute and add sample to Standard: set 10 Standard wells on the ELISA pre-coated plates, add Standard 100μl to the first and the second well, then add Standard dilution 50μl to the first and the second well, mix; take out 100μl form the first and the second well then add it to the third and fourth well separately. then add Standard dilution 50μl to the third and the forth well ,mix ; then take out 50μl from the third and the forth well discard, add 50μl to the fifth and the sixth well ,then add Standard dilution 50μl to the fifth and the sixth well, mix ; take out 50μl from the fifth and the sixth well and add to the seventh and the eighth well, then add Standard dilution 50μl to the seventh and the eighth well ,mix ; take out 50μl from the seventh and the eighth well and add to the ninth and the tenth well, add Standard dilution 50μl to the ninth and the tenth well, mix , take out 50μl from the ninth and the tenth well discard(add Sample 50μl to each well after diluting.

Added sample, set blank wells separately (blank comparison wells don't add sample and HRP Conjugate reagent, other each step operation is same) testing sample well. Add Sample dilution 40μl to testing sample well, then add testing sample 10μl (sample final dilution is 5-fold), add sample to wells, don't touch the well wall as far as possible, and gently mix. Incubate after closing plate with Closure plate membrane, incubate for 30 min at 37^{o}C. Configurate liquid: 30-fold (or 20-fold) wash solution diluted 30-fold (or 20-fold) with distilled water and reserve. Washing Uncover Closure plate membrane, discard Liquid, dry by swing, add washing buffer to every well, still for 30s then drain, repeat 5 times, dry by pat. Add enzyme Add HRP-Conjugate reagent 50μl to each well, except blank well. Incubate, Operation with 3and Washing operation with as step as above. Add Chromogen Solution A 50ul and Chromogenic Solution B to each well, evade the light preservation for

15 min at 37^{o}C. Stop the reaction, Add Stop Solution50μl to each well, Stop the reaction (the blue color change to yellow color). Assay takes blank well as zero, read absorbance at 450nm after Adding Stop Solution and within 15min. Note the absorbance values, constructed the Standard curve and calculated sample protein concentrations based on absorbance values.

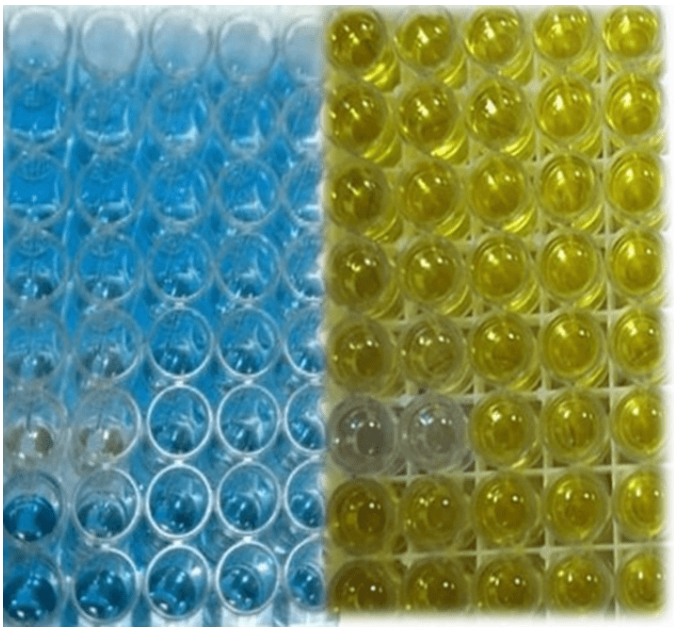

FIGURE 3.14: Primary coated antibody 96 well plates used in ELISA assay.

Figure 3.14 shows 96-well microplates already coated with primary antibodies that were specific to TNF-α. In the ELISA procedure, the samples and standards can be added to the wells, and TNF-α can bind to the antibodies, and then be detected using an enzyme-linked method that shows quantitatively. (Photograph taken at faculty of Pharmacy, Capital University of Science and Technology).

3.12 Molecular Docking

Molecular docking is a computational approach for the simulation and investigation of drug interactions with its biological target at the level of molecular structure. This approach enables the assessment of a number of different parameters to provide valuable insight into the binding of NSAIDs to the active sites of COX enzymes. Parameters such as binding free energy and inhibition constants are examples of

molecular docking parameters. Molecular docking is a structure-based drug design tool that can imitate the molecular interaction and provide a prediction of binding mode and affinity between ligand and receptor.

Molecular docking is, imitate the best conformation in accordance with complementarity as well as pre-organization to predict and retrieve the binding affinity and interactive mode between ligand and receptor.

This study has made use of a variety of computational tools, including PyMOL™3.0.4, AutoDock tools-1.5.7, Discovery Studio 2017 R2 client, and ChemDraw. ChemDraw was used to depict the chemical structures of selected compounds.

Molecular docking studies were conducted using AutoDock and Discovery Studio to predict the binding interaction of specific chemical compounds with multiple target proteins. The three-dimensional (3D) and two-dimensional (2D) structures of the substituted compounds were generated using Discovery studio.

Molecular docking studies were conducted using AutoDock tool, targeting the protein structure. Discovery Studio Visualizer was employed to analyze the binding interactions and identify the most favorable binding conformations, based on lower binding free energy. Key amino acid residues involved in ligand-protein interactions were further analyzed through both 3D and 2D visual representations.

These methods allowed for the prediction and visualization of molecular interactions and provided a means to use binding affinities and possible mechanisms of action. Ibuprofen used as reference (standard) and Etoricoxib were included for comparisons.

3.12.1 Ligands Preparation

ChemDraw tool was used for ligand structures base construction. The structures were saved as mol files, were optimized by using discovery studio software and then saved in .pdb format. Then, AutoDockTools-1.5.6 was used to convert the files in .pdbqt format.

3.12.2 Proteins Preparation

The target protein structures were captured against various receptors COX2, TNF-α and NF-κB by using PDB ID: 4ph9, 2az5 and 9bdw from PDB (Protein Data Bank) (http://www.rcsb.org). Discovery Studio Visualizer was used to remove the solvent and native ligand from the crystal. The proteins were saved as .pdb files. AutoDockTools-1.5.6. was used to add polar hydrogen to the protein structure and to save data as .pdbqt files.

The COX-2 protein structure (PDB ID:4ph9) was retrieved from the Protein Data Bank, to prepare the protein for docking simulations, removed unnecessary water molecules and other non-essential elements. Hydrogen atoms were added to stabilize the molecular structure and enable more accurate predictions of ligand binding interactions. The processed protein structure was saved in .pdbqt format, suitable for docking simulations.

The docking grid was configured to include key residues in the COX-2 active site, identified from previous structural studies as ALA B157, HIS B 341, and PRO B35. The grid dimensions were set at 126x126x126 Åwith a grid spacing of 0.689 Å, ensuring comprehensive binding site coverage. The grid box was centered at x = 20.727, y = 25.501, and z =48.427 to capture all potential binding interactions between the ligands and the enzyme's active site residues.

The TNF-α protein structure (PDB ID:2az5) was retrieved from the Protein Data Bank. The grid dimensions were set at 84x94x80 Åwith a grid spacing of 0.700 Å, ensuring comprehensive binding site coverage. The grid box was centered at x = -19.364 y = 65.266, and z =32.431 to capture all potential binding interactions between the ligands and the enzyme's active site residues.

The NF-κB (PDB ID:9bdw) was retrieved from the Protein Data Bank. The grid dimensions were set at 62x62x62 Åwith a grid spacing of 0.660 Å, ensuring comprehensive binding site coverage. The grid box was centered at x = -68.002 y= -9.250, and z =-18.222 to capture all potential binding interactions between the ligands and the enzyme's active site residues.

3.13 Evaluation of Liver Histopathological Changes

For morphometric evaluation, the liver tissues were first fixed in 10% formalin, which preserves the cellular architecture, then went through a process of being boxed in paraffin blocks before being sectioned. The sections were cut at lengths of 5μm using a microtome. The sections were stained with hematoxylin and eosin (H&E) to evaluate general histological features as well as with Masson's trichrome stain to evaluate collagen deposition. The staining procedures followed standard, established procedures for histological evaluations.

Histological staining was performed with the H&E method for examining tissue architecture and pathology. H&E is a popular method for general tissue morphology. Tissues were fixed, processed and embedded in paraffin wax in a standard manner, with fixation of tissues in 10% neutral-buffered formalin for 24-48 hours at room temperature to preserve morphology. Samples that were embedded in paraffin wax were sectioned on a rotary microtome to make 4-5 μm slides. The sections were mounted on clean glass microscope slides to dry overnight at 37^{o}C for 1 hour to increase adhesion before staining. First, the slides were deparaffinized in xylene (2 changes of 5 minutes each). After deparaffinization for morphometric evaluation, the liver tissues were first fixed in 10% formaldehyde, which preserves the cellular architecture, then went through a process of being boxed in paraffin blocks before being sectioned. The sections were cut at lengths of 5μm using a microtome. The sections were stained with hematoxylin and eosin (H&E) to evaluate general histological features as well as with Masson's trichrome stain to evaluate collagen deposition and therefore fibrosis. The staining procedures followed standard, established procedures for histological evaluations. For morphometric evaluation, the liver tissues were first fixed in 10% formaldehyde, which preserves the cellular architecture, then went through a process of being boxed in paraffin blocks before being sectioned. The sections were cut at lengths of 5μm using a microtome. The sections were stained with hematoxylin and eosin (H&E) to evaluate general histological features as well as with Masson's trichrome stain to evaluate collagen deposition and

therefore fibrosis. The staining procedures followed standard, established procedures for histological evaluations., they were rehydrated in a descending series of alcohol (100%, 95%, and 70% ethanol) and were rinsed briefly in distilled water. The sections were then stained in Harris's hematoxylin solution for 5-7 minutes to visualize the nuclei of cells, followed by rinsing in running tap water to remove excess stain. Differentiation was performed, if necessary, in 1% acid alcohol (1% HCl in 70% ethanol) for a few seconds to remove non-specific nuclear staining and bluing of nuclei was performed by immersing in 0.2% ammonia water or alkaline tap water for 1 minute. The cytoplasmic and extracellular components were counter-stained in 1% eosin Y solution for 30 seconds - 1 minute, and after eosin staining the slides were rinsed in distilled water rapidly to avoid overstaining. The stained sections were dehydrated through an ascending alcohol series (70%, 95%, and 100%), then cleared in xylene (2 changes, 3 minutes each). Coverslips were mounted using a xylene-based permanent mounting medium to preserve the stained sections. The stained slides then dried thoroughly and were examined under a bright-field light microscope using various magnifications (10x, 40x) to assess cellular morphology, organization of tissues, and any histopathological changes, with representative images captured for record keeping and analysis.

3.14 Statistical Analysis

Quantitative data were expressed as mean ± standard deviation (SD). Statistical analysis was performed using Graph Pad Prism 8.0.1 software (GraphPad Software Inc., San Diego, CA, USA). One-way analysis of variance (ANOVA) followed by post hoc Turkey's multiple comparison test was employed for detection of differences among experimental groups, p-value of < 0.05 was considered a measure of statistical significance. Standard curves were obtained by linear regression, and the corresponding concentrations of TNF-α were read off from sample absorbance values for ELISA and BCA assay data. Each experimental group consisted of n = 6 animals to ensure sufficient statistical power.

Chapter 4

Results

This chapter presents the experimental results from the study, investigating the hepatoprotective and anti-inflammatory effects of etoricoxib and ibuprofen in a mice model of ethanol-induced hepatotoxicity. Inflammatory biomarker levels were measured using an ELISA based method, in order to determine the biomarker values referenced to a standard curve. The results were discussed in relationship to the dose-dependent effects of the research compounds and mechanistic relevance of the research compounds in relation to ethanol-induced hepatotoxicity. In our study, we described a mice model of ethanol-induced hepatotoxicity to study the potential therapeutic effect of the etoricoxib selective COX-2 inhibitor and ibuprofen non-selective COX-2 inhibitor.

4.1 Biochemical Markers of Hepatic Injury

In the current study, mice model of ethanol induced hepatotoxicity blood was collected via cardiac puncture in a sterile manner and processed for serum biochemistry. Serum ALT and AST activities were measured using standard enzymatic colorimetric detection methods by a certified diagnostic laboratory. The high serum

markers after ethanol treatment are indicative of significant hepatic stress, membrane disruption, and hepatocellular injury. The biochemical disruption is consistent with ethanol-induced hepatotoxicity. After the treatment phase of the study, administration of the selective COX-2 inhibitor, etoricoxib at (50 mg/kg) showed a stronger hepatoprotective effect while still representing the dose-response profile. We observed to reduce elevated liver enzymes. These findings are consistent with COX-2 selective inhibition as anti-inflammatory. Etoricoxib both at low (25 mg/kg) and high dose (50 mg/kg) doses), or non-selective NSAID ibuprofen (50 mg/kg) led to significant reduction in serum transaminase ALT and AST levels, indicating an improvement in hepatic function and membrane stability, suggesting some potential for hepatoprotective agents that might ameliorate ethanol-induced liver pathology.

4.2 Serum Alanine Aminotransferase and Serum Aspartate Aminotransferase Levels

ALT is a very sensitive measure of liver damage. The serum ALT levels of the ethanol-only group rise significantly compared to controls group, indicating liver damage was severe. Treatment with etoricoxib at both doses (low dose 25mg/kg and high dose (50 mg/kg)) and standard reference ibuprofen 50mg/kg significantly reduced ethanol injured ALT levels indicating hepatoprotective effect against hepatic injury.

The control group had an ALT level of 45 $\pm$ 2.5 U/L. Administration of ethanol, at a dose of (5 g/kg), resulted in a significantly higher ALT at 170 $\pm$ 5.0 U/L (#p $<$ 0.05 vs control). Treatment with ibuprofen (50 mg/kg) significantly lowered ALT levels to an average of 75 $\pm$ 3.5 U/L (*p $<$ 0.001 vs ethanol group). At a dose of (25 mg/kg), etoricoxib lowered the ALT levels to 130 $\pm$ 2.8 U/L (*p $<$ 0.001 vs ethanol), while (50 mg/kg) further lowered ALT to 60 $\pm$ 2.1 U/L (***p $<$ 0.001 vs ethanol), closer to normal levels. Ethanol administration resulted in ALT levels that significantly exceeded those observed in the control group, a confirmation of hepatocellular damage.

Etoricoxib treatment significantly reduced ALT levels in a dose-dependent manner, with the (25 mg/kg) etoricoxib reducing ALT by 29.3%, and the (50 mg/kg) by 48.2% when compared to the ethanol group. While ibuprofen reduced ALT by 34.5% when compared to ethanol, the doses of etoricoxib (50 mg/kg) proved to be the best option for hepatoprotection.

Aspartate aminotransferase (AST) is another marker of injury to liver and systemic cells. An increase in AST indicates hepatocellular damage.

The ethanol group have a raised in AST level in blood. As observed, both etoricoxib and ibuprofen reactively reduced the raised AST levels caused by ethanol. Etoricoxib was more effective especially at a higher dose.

The normal control group had an AST level of 32 ± 2.0 U/L. Ethanol administration (5 mg/kg) significantly elevated AST to 127 ± 4.0 U/L (#p $<$ 0.05 vs. control). Ibuprofen (50 mg/kg) treatment significantly decreased AST to 57 ± 3.0 U/L (*p $<$ 0.001 vs. ethanol).

Etoricoxib at (25 mg/kg) reduced AST to 90 ± 1.9 U/L (p $<$ 0.01 vs. ethanol), while the (50 mg/kg) dose further normalized AST levels to 45 ± 3.2 U/L (****p $<$ 0.001 vs. ethanol), comparable to the control group.

The AST levels were significantly elevated in the ethanol group, showing evidence of hepatocellular injury. Treatment with etoricoxib at (25 mg/kg) and at (50 mg/kg) attenuated the AST levels by 29.2% and 48.5%, respectively, while ibuprofen produced a reduction of 32.8%.

Based on these findings, it is established that higher dose etoricoxib provides better prevention against ethanol-induced hepatic damage.

Figure 4.1 represent the serum ALT levels were significantly elevated in the ethanol-treated group (5 g/kg) compared to the control group, indicating liver damage (### p $<$ 0.001 vs. control). Treatment with Etoricoxib at (25 mg/kg) and (50 mg/kg), as well as Ibuprofen at (50 mg/kg), significantly reduced ALT levels compared to the ethanol group (*** p $<$ 0.001 vs. ethanol).

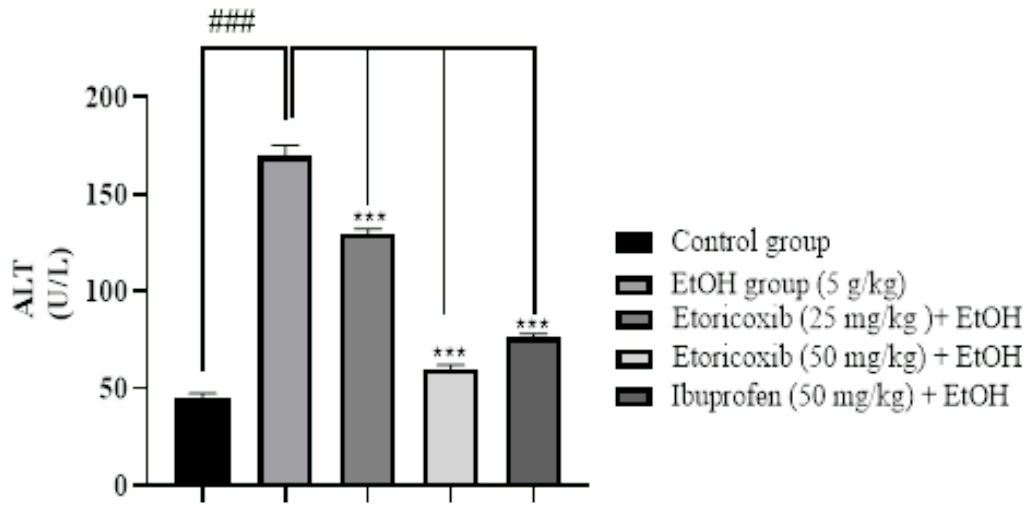

FIGURE 4.1: Serum alanine transaminase levels in ethanol-induced liver injury in mice.

Data are expressed as mean ± SD (n = 6 per group). Statistical analysis was performed using one-way ANOVA followed by Tukey's post hoc test.

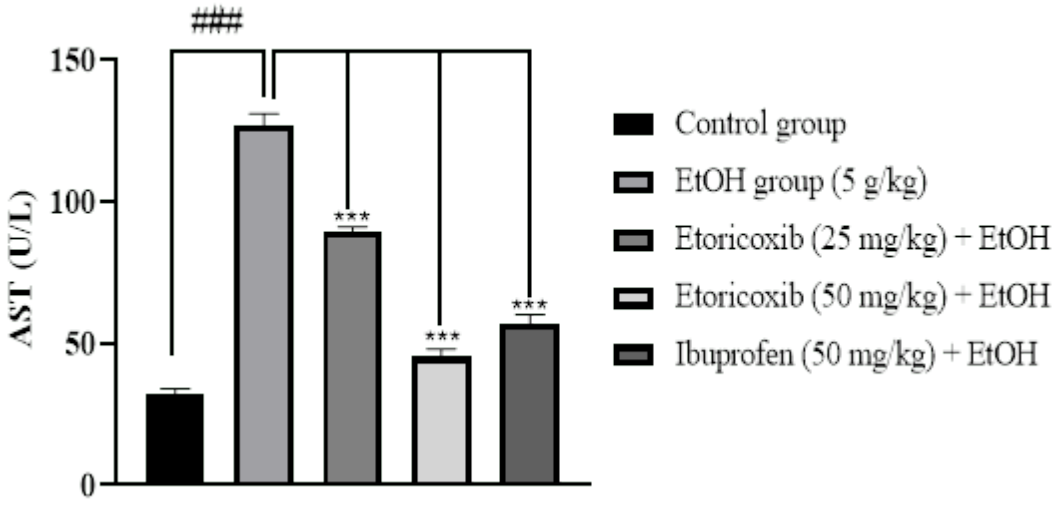

FIGURE 4.2: Serum aspartate transaminase levels in ethanol-induced liver injury in mice.

Figure 4.2 demonstrates serum AST values which were significantly elevated in the ethanol-treated (5 g/kg) with respect to the control which signifies hepatocellular damage (### p <0.001 vs control). Treatment with Etoricoxib at (25 mg/kg) and (50 mg/kg), and Ibuprofen at (50 mg/kg) significantly decreased AST values with respect to the ethanol group (*** p <0.001 vs ethanol). Data expressed as

mean ± SD (n = 6 per group). Data analysed by one-way ANOVA and analysed for statistical difference with Tukey's post hoc test.

4.3 Inflammatory Marker Analysis

After collecting blood via cardiac puncture, the mice were sacrificed, and livers were excised. The liver tissues were then stored in PBS, pH 7.4 for biochemical analysis. BCA assay was performed to measure protein concentration and then Elisa was performed for quantification of TNF-α.

4.3.1 BCA Protein Assay Protocol

Absorbance was read at 562 nm, and concentrations were determined from a standard curve consisting of known protein concentration. Standard Curve for protein concentration ranging from 0 to 20 μg/μl was generated and the absorbance values at 562 nm were used to create the linear regression equation in order to extrapolate the concentration from unknown samples.

The concentration of total protein in liver tissue homogenates was determined using the BCA assay to assess hepatocellular integrity following ethanol-induced liver injury and pharmacological treatment. The normal control group had an average protein concentration of 8.42 ± 0.30 μg/μL, which is indicative of normal hepatic homeostasis. Ethanol (5 mg/kg) administration, total protein concentration increased significantly to 18.33 ± 0.64 μg/μL, which was indicative of significant hepatic inflammation and tissue damage.

The increase in total protein concentration likely resulted from increased cellular permeability which is characterized by protein leaking into the extracellular matrix. Treatment with etoricoxib at (25 mg/kg) resulted in a reduction in protein concentration to 16.19 ± 0.83μg/μL suggesting a moderate hepatoprotective activity. Etoricoxib (50 mg/kg) produced a greatest reduction in total protein concentration 14.49 ± 0.87μg/μL and was approaching near-normal values while still providing

additional protection, in a concentration-dependent manner. Ibuprofen lowered the total protein concentration to 15.89 μg/μL, indicating anti-inflammatory activity, while suggesting less efficacious than the higher dose of etoricoxib.

Taken together, and at the very least based on the total protein measure, etoricoxib offered significant protection against ethanol-induced hepatic protein dysregulation, likely mediated by COX-2 inhibition and the inhibition of other inflammatory signaling.

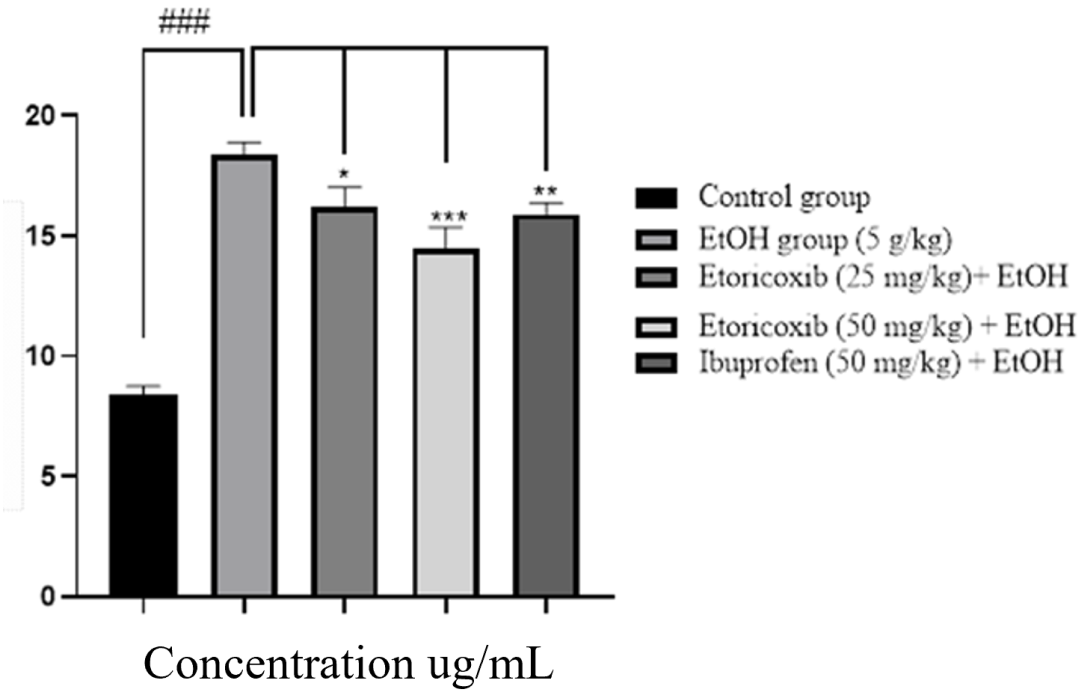

FIGURE 4.3: BCA assay, protein concentration in experimental group.

Figure 4.3 shows protein concentrations, which were significantly elevated in the ethanol-treated group (5 g/kg) relative to the control group, indicating possible hepatic dysfunction (### $p < 0.001$ vs. control). Treatment with Etoricoxib at (25 mg/kg) or (50 mg/kg) (along with Ibuprofen at (50 mg/kg) significantly decreased protein concentrations compared to ethanol (* $p < 0.05$, ** $p < 0.01$, *** $p < 0.001$ vs. ethanol).

Data were expressed as means $\pm$ SD ($n = 6$ per group). Statistical analysis consisted of one-way ANOVA with Tukey's post hoc test.

4.3.2 TNF-α levels

The standard curve was established and demonstrated a high degree of linearity ($R^2 \geq 0.99$), which confirmed the sensitivity and reliability of the assay for quantifying TNF-α in the current range. The sample concentrations were interpolated from the standard curve after background absorbance was deducted. The method used ensured accurate measurements of TNF-α levels reflecting the degree of hepatic inflammation due to ethanol administration, along with the anti-inflammatory action of etoricoxib and ibuprofen.

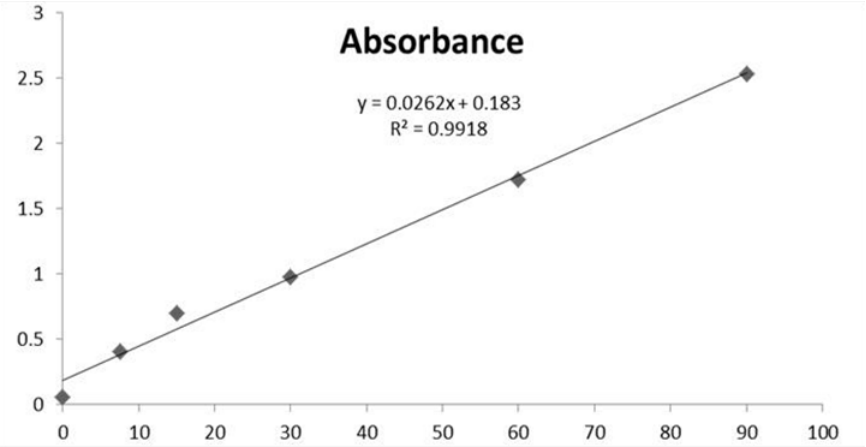

FIGURE 4.4: Standard curve for TNF-α.

Standard curve generated for ELISA quantification of protein. Known concentrations of the standard were plotted against their corresponding optical density (OD) values at 450 nm. The curve demonstrates a linear relationship ($R^2 = 0.99$), enabling accurate interpolation of sample concentrations within the dynamic range of the assay.

4.3.2.1 TNF-α Levels in Experimental Groups

In mice model of ethanol induced hepatoxicity, inflammatory biomarker levels were quantified using an ELISA-based method, and group-wise to estimate biomarker concentrations with reference to a standard curve. The results were discussed with respect to the dose-dependent effects of the test compounds and their mechanistic relevance in mitigating ethanol-induced liver injury. Ethanol 5g/kg administration

caused an increase in expression TNF-α in the liver compared to the intact control group. Etoricoxib (low dose) (25mg/kg) + (ethanol 5g/kg) group post administration of ethanol down regulated the expression of TNF-α, but etoricoxib (high dose) (50 mg/kg) + ethanol (5 g/kg) group yield relative better result. Ibuprofen (50mg/kg) + ethanol (5 g/kg) group also shows reduction in levels of TNF-α but it has less effect than etoricoxib (50 mg/kg). Administration of etoricoxib (25 mg/kg), etoricoxib (50 mg/kg) and ibuprofen 50mg/kg in three groups caused a significant decrease in the levels of TNF-α compared to the groups that received ethanol only. This study assesses the anti-inflammatory potential treatments in suppressing TNF-α levels compared to ethanol-induced expression. Ethanol treatment resulted in a significant increase in tissue TNF-α levels suggesting an inflammatory reaction. Etoricoxib at (25 mg/kg) and (50 mg/kg) reduced TNF-α levels by approximately 31.6% and 44.5%, respectively, compared with ethanol and ibuprofen at the same concentration reduced TNF-α levels by 33.8% compared to ethanol. Absorbance readings were taken at 450 nm and plotted a standard regression equation, which was then used to extrapolate TNF-α concentration in liver tissue lysate samples. TNF-α concentration were calculated from the absorbance values for each sample as obtained from the standard curve.

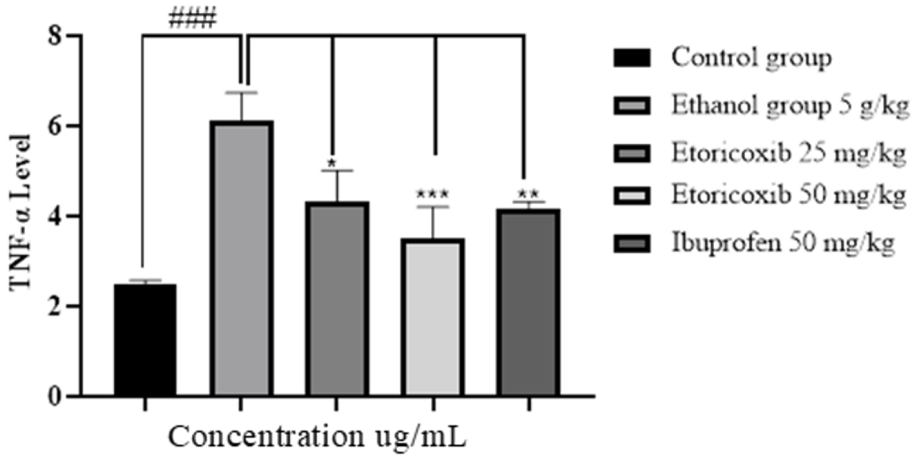

FIGURE 4.5: TNF-α concentration in experimental group by ELSIA.

Figure 4.5 graph TNF-α levels; animals given ethanol (5 g/kg) had an elevated TNF-α level compared to the control, indicating an inflammatory response (### $p < 0.001$ vs. control). Animals administered Etoricoxib (25 mg/kg) and (50 mg/kg))

or Ibuprofen (50 mg/kg) had significantly lower levels of TNF-α Tukey's post-hoc test, * $p < 0.05$, ** $p < 0.01$, *** $p < 0.01$) compared to the ethanol treatment. Data were presented as mean ± SD (n = 6 per group) and analyzed by one-way ANOVA, followed by Tukey's post hoc test. Administration of ethanol (20% v/v), (5 g/kg) significantly increased TNF-α expression in liver tissue of the test group versus the control group, confirming ethanol-induced hepatic inflammation. The average absorbance values for TNF-α expressed by the ethanol-treated group (6.17 ± 0.69) were significantly increased from the average values for the control group (2.48 ± 0.10). This result is consistent with the identified upregulation of the TNF - α pro - inflammatory cytokine. We have documented TNF-α in the context of ethnol-induced liver injury, where TNF-α signaling will elicit pro-inflammatory activity to promote inflammation to assist in the eradication of the ethanol while allowing for chronic hepatocyte apoptosis that leads to fibrotic temples of liver injury.

The administration of etoricoxib (25 mg/kg) in the context of ethanol treatment reduced the values of TNF-α (4.30± 0.71), meaning that (25 mg/kg) of etoricoxib demonstrated partial anti-inflammatory efficacy. The administration of etoricoxib (50 mg/kg) in the context of ethanol treatment also reduced the absolute values of TNF-α (3.48 ± 0.71) and indicated that the dose of etoricoxib may suppress TNF-α levels in a dose dependent inhibition of ethanol-induced inflammation. In our examination this data supports the hypothesis that higher doses of selective COX-2 inhibitors, etoricoxib may be more effective in the attenuation of inflammatory cytokine production in mice models of hepatotoxicity. For comparison, even though ibuprofen (50 mg/kg) (4.14 ± 0.17). Had a similar anti-inflammatory effect, it was not as effective at the dose examined as etoricoxib at (50 mg/kg). Because Ibuprofen is a non-selective COX inhibitor (inhibiting both COX-1 and -2), it may have limited the specificity of its anti-inflammatory effect when compared to etoricoxib which suppressed COX-2 expression through inhibition and was focused on a specific enzyme of attenuation. These findings are consistent with the previously accepted action of COX-2 inhibition to modulate cytokine-mediated inflammatory pathways, indicating that selective COX-2 inhibitors (such as etoricoxib) may represent a more favorable pharmacological approach than non-selective NSAIDs in

alcohol-associated liver disease.

4.4 Molecular Docking Analysis

Molecular docking analysis revealed distinct differences in the binding affinities and interaction profiles of selective etoricoxib and nonselective ibuprofen with COX-2, TNF-α and NF-κB.

4.4.1 Molecular Docking Analysis of Etoricoxib Compound at Different Cytokines Receptor

Among the tested ligands, etoricoxib demonstrated the highest docking score, indicating a relatively stronger binding affinity. Etoricoxib form stable complexes with COX-2, TNF-α, Nf κb. The docking scores of the ligands with (Cox2 -8.9 kcal/mol, TNF-α-8.3 kcal/mol, NF-κB -6.3 kcal/mol shown in table 4.1.

TABLE 4.1: Binding affinities of etoricoxib with receptors

Sr. No	Target protein	PDB ID	Binding affinities kcal/mol
1	COX-2	4ph9	-8.9
2	TNF-α	2az5	-8.3
3	NF-κB	9bdw	-6.3

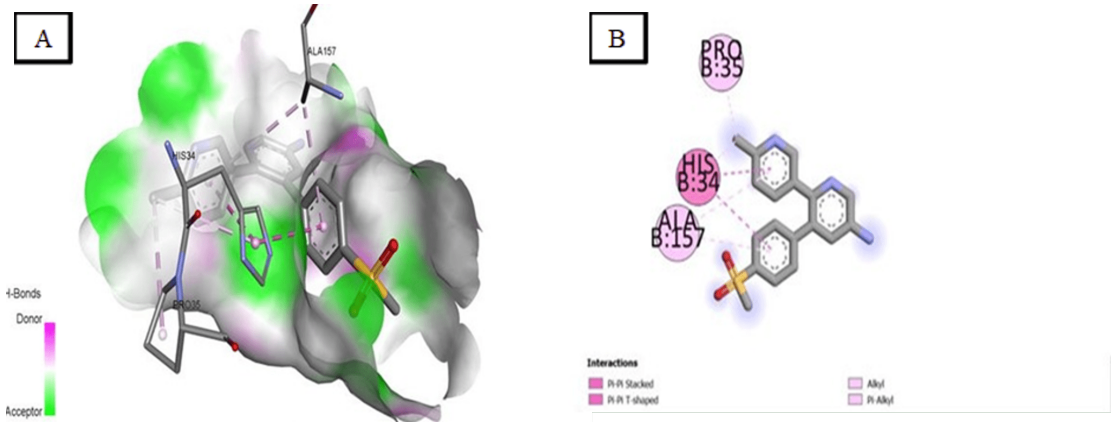

FIGURE 4.6: 3D and 2D visualization of interaction with amino acid residues of the COX-2 active site with ligand etoricoxib.

The figure A shows 3D interaction of etoricoxib, which has a deep binding within the COX-2 active site. This is stabilized hydrogen bond with Arg120 and Tyr355. Forms hydrogen bonds with the sulfonyl group of the ligand (the sulfonamide moiety).

Hydrophobic interactions of the ligand with Val349 and Leu352 additionally stabilizes the complex.

The figure B 2D interaction, sulfonamide group has a strong hydrogen bond with Arg120 and the methyl group on the pyridine ring has van der Waals contacts with Leu352.

The phenyl ring has a π-π stack with Tyr355 which enables specificity of binding.

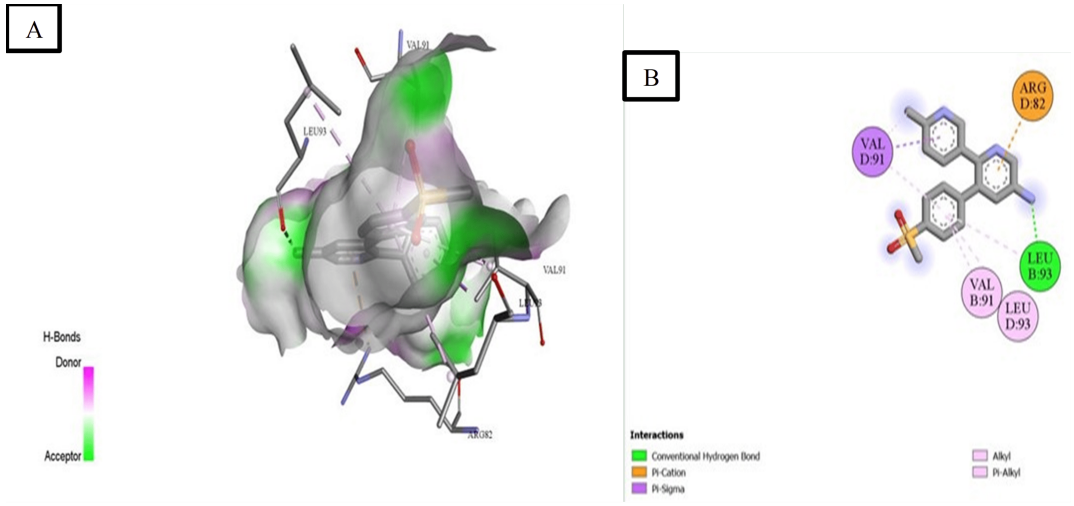

FIGURE 4.7: 3D and 2D visualization of interaction with amino acid residues of the TNF-α active site with ligand etoricoxib.

The figure A shows 3D interaction of etoricoxib, fits into a small gap close to the TNF-α trimer interface and forms hydrophobic interactions with Leu57 and Tyr119, and the structured sulfonyl oxygen from the ligand hydrogen bond to the backbone NH of Tyr119.

The figure B 2D interaction, pyridine ring interacts with Leu57 through hydrophobic interactions while the sulfonamide group interacts with Tyr119 by hydrogen bonding, and there are minor van der Waals contacts with Gly121 and Val123 which likely contribute to stability.

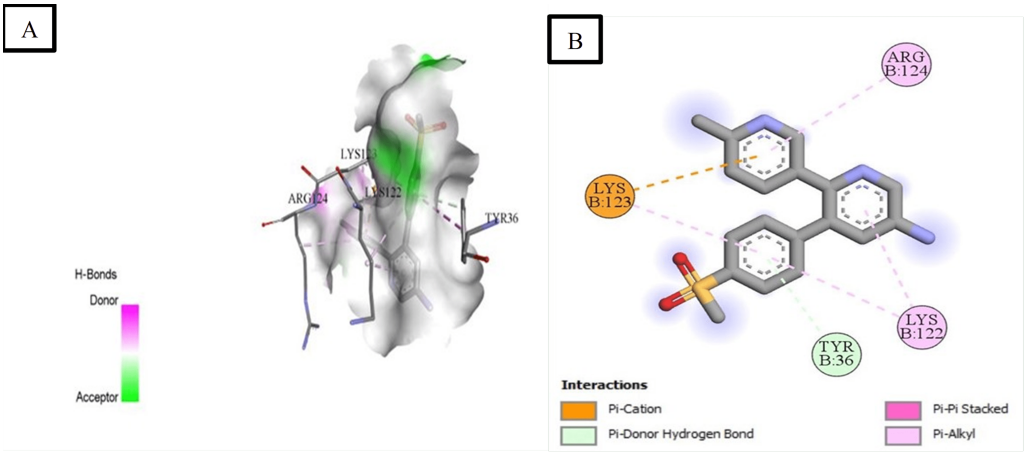

FIGURE 4.8: 3D and 2D visualization of interaction with amino acid residues of the NF-κB active site with ligand etoricoxib.

The figure A shows 3D interaction etoricoxib binds into a regulatory site near the DNA-binding domain of NF-κB, primarily with van der Waals interactions with Lys145 and Arg307. There are not many significant hydrogen bonds.

The figure B 2D interaction chlorophenyl group of the ligand fits into a hydrophobic pocket formed by Ile165 and Val248, while the sulfonamide group weakly polarizes Arg307.

The molecular docking analysis of etoricoxib against key inflammatory targets COX-2 TNF-α, NF-κB, revealed significant binding affinities, suggesting its potential for multi-target anti-inflammatory action. These results indicate that etoricoxib has the strongest binding affinity for COX-2, which aligns with its established pharmacological role as a selective COX-2 inhibitor. The interaction with TNF-α was also notably strong, highlighting potential additional mechanisms in inflammation suppression. In contrast, while the docking score with NF-κB was slightly lower, it still reflects a meaningful interaction that may contribute to the compound's broader anti-inflammatory activity.

Three-dimensional (3D) structural analysis showed that etoricoxib fits well into the active binding pockets of all three proteins. In the COX-2 complex, the ligand formed stable interactions through hydrogen bonds with key residues such as Arg120 and Tyr355, as well as hydrophobic contacts with Val349 and Leu352.

The TNF-α complex revealed hydrophobic interactions within a surface cleft, involving residues like Leu57 and Tyr119. For NF-κB, the ligand was accommodated in a regulatory region, stabilized mainly by van der Waals forces with limited hydrogen bonding.

Two-dimensional (2D) interaction diagrams further supported these findings, particularly in the COX-2 complex, where hydrogen bonding, π-π stacking, and hydrophobic interactions were prominently observed, confirming the specificity and stability of the ligand binding.

Overall, the docking analysis demonstrates that etoricoxib not only retains strong affinity for its known target, COX-2, but also shows potential for modulating TNF-α and NF-κB, which could enhance its therapeutic effectiveness in inflammatory conditions.

4.4.2 Molecular Docking Analysis of Ibuprofen Compound at Different Cytokines Receptor

Ibuprofen has formed stable complexes with COX-2, TNF-α, and NF-κB, although it has a lower affinity for the proteins than etoricoxib.

We measured ibuprofen's dock score the greater the number, the stronger the interactive binding energies to these proteins as follows: at COX-2 (-7.0 kcal/mol) and TNF-a (-6.9 kcal/mol) its interaction was moderate; with NF-κB the interaction was weaker at (-5.4 kcal/mol) shown in table 15.

Overall, ibuprofen displayed weaker molecular interactions with these targets ultimately than the etoricoxib.

Table 4.2: Binding affinities of ibuprofen with receptors

Sr. No	**Target protein**	**PDB ID**	**Binding affinities kcal/mol**
1	Cox2	4ph9	-7
2	TNF-α	2az5	-6.9
3	NF-κB	1vkx	-7.8

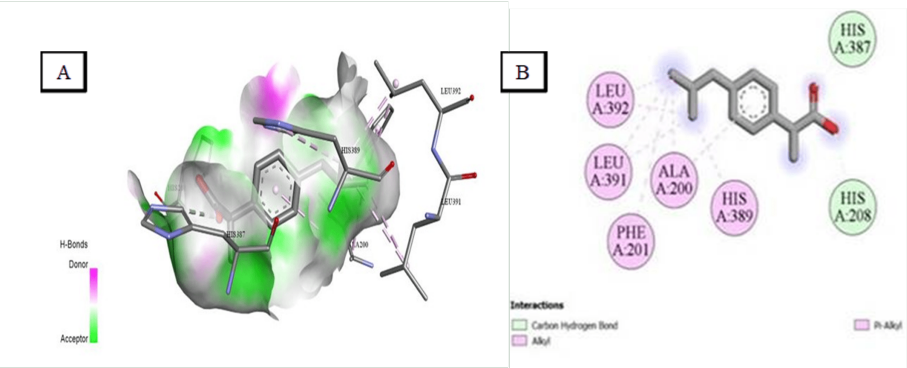

FIGURE 4.9: 3D and 2D visualization of interaction with amino acid residues of the COX-2 active site with ligand ibuprofen.

The figure A shows 3D interaction of ibuprofen interacts nearby the COX-2 catalytic site, where there is a hydrogen bond between the carboxylate group of ibuprofen and Arg120. The isobutyl group has hydrophobic interactions with Leu352 and Val349. The above figure B shows 2D interaction, Hydrogen bond between the carboxylic acid group with Arg120, and π-alkyl interactions of the phenyl ring with Leu352; have weak van der Waals interactions with Tyr385.

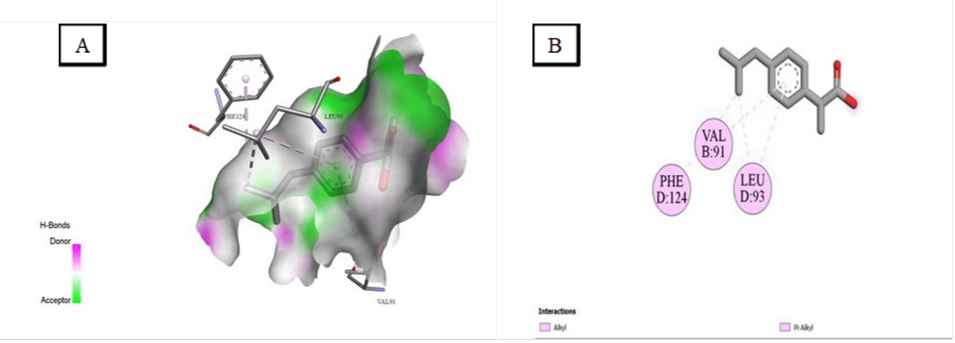

FIGURE 4.10: 3D and 2D visualization of interaction with amino acid residues of the COX-2 active site with ligand ibuprofen.

The figure A shows 3D interaction of ibuprofen bind in a shallow manner to TNF-α through hydrophobic interactions involving Leu57 and Tyr119. There is no hydrogen bonding interaction observed.

The figure B shows 2D interaction, propionic acid group is solvent exposed and the phenyl ring is placed in a shallow pocket formed by Leu57 and Tyr119.

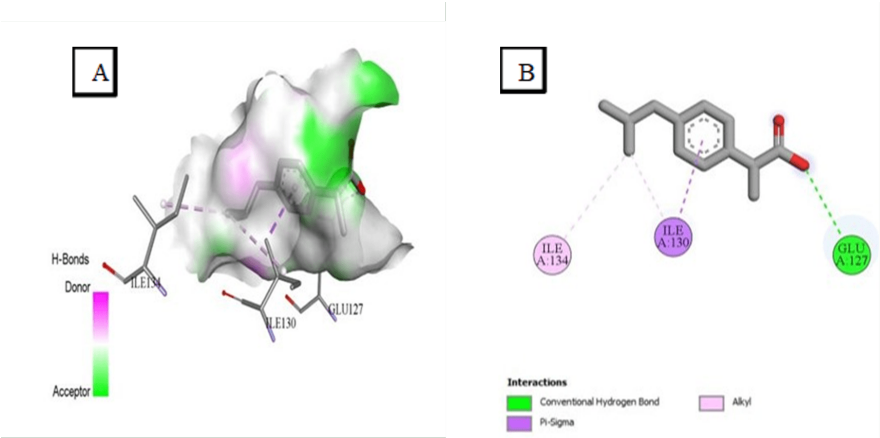

FIGURE 4.11: 3D and 2D visualization of interaction with amino acid residues of the NF-κB active site with ligand ibuprofen.

Figure 4.11 A shows 3D interaction of ibuprofen has a weak association with the minor groove of NF-κB primarily via Van der Waals interactions with Lys145 and Arg307.

The figure B shows 2D interaction, carboxylate of the ligand forms a salt bridge with Arg307.

The molecular docking study of ibuprofen with COX-2, TNF-α, and NF-κB showed its potential to stabilize protein-ligand complexes with these proteins although it did have slightly lower binding affinities than etoricoxib. The docking scores for ibuprofen were -7.0 kcal/mol with COX-2, -6.9 kcal/mol with TNF-α, and -5.4 kcal/mol with NF-κB, the scores indicate a binding potential in the moderate to good range especially for COX-2 and TNF-α. In accordance with ibuprofen being a non-selective NSAID, it can potentially interact with multiple inflammatory mediators. Although it was less than etoricoxib, the reportedly reflects a meaningful interaction of ibuprofen with the inflammatory cascade. Three-dimensional (3D) structural visualization showed ibuprofen appropriately fits within the active binding pockets of each of the three proteins. In the COX-2 complex (PDB ID: 4PH9), ibuprofen was incorporated by hydrogen bonds and hydrophobic interactions with amino acid residue essentially yellowing stabilization of the binding pattern of ibuprofen while in the cyclooxygenase catalytic domain (Figure 4.10). The TNF-α complex (PDB ID: 2AZ5) showed sufficient hydrophobic interactions with

Leu57 and Tyr119 residues anchoring the ligand in a cleft that was accessible to the surface, establishing a binding interaction between the two (Figure 4.11). In the case of NF-κB (PDBID:1VKX), ibuprofen seemed to exhibit lower docking scores, specifically stabilization due to vanvander Waals contacts leading to an unstable interaction.

4.5 Histopathological Changes in Ethanolic Liver Injury due to Etoricoxib Administration

The morphological arrangement of liver cells in the normal control group showed healthy signs with regular hepatocyte arrangements, distinct nucleus, and sinusoids. In contrast, the hepatocytes of the ethanol-induced model group showed extensive disarrangement with loss of sinusoidal spaces, inflammatory signs with in cells, infiltrations were observed.

Necrotic cells were found with loss of nuclear integrity, ballooning degeneration, and fatty changes were clearly visible caused by ethanol-induced liver damage. The etoricoxib treated group showed positive morphology of liver with arrangement of hepatocytes almost similar to normal liver. By restoring the hepatocyte arrangements, reduced inflammatory cell infiltration, and preserved sinusoidal spaces. H&E staining of ethanol-induced liver damage and the protective effects of etoricoxib at 40× magnification.

Figure 4.12 shows H&E staining of ethanol-induced liver damage and the protective effects of etoricoxib at 40× magnification. Control group shows normal arrangement of hepatocytes and sinusoidal spaces, ethanol group shows heavy loss of sinusoidal spaces, presence of necrotic cells, lymphocytic infiltration, ballooning degeneration, changes were observed, indicated by black arrows, etoricoxib (25 mg/kg + EtOH) group shows several necrotic hepatocytes and lymphocytic infiltrations present, indicated by black arrows but mostly sinusoidal spaces show recovery, etoricoxib (50 mg/kg + EtOH) group shows hepatocytes signs of protection against ethanol-induced liver injury with distinct sinusoidal spaces, and ibuprofen group

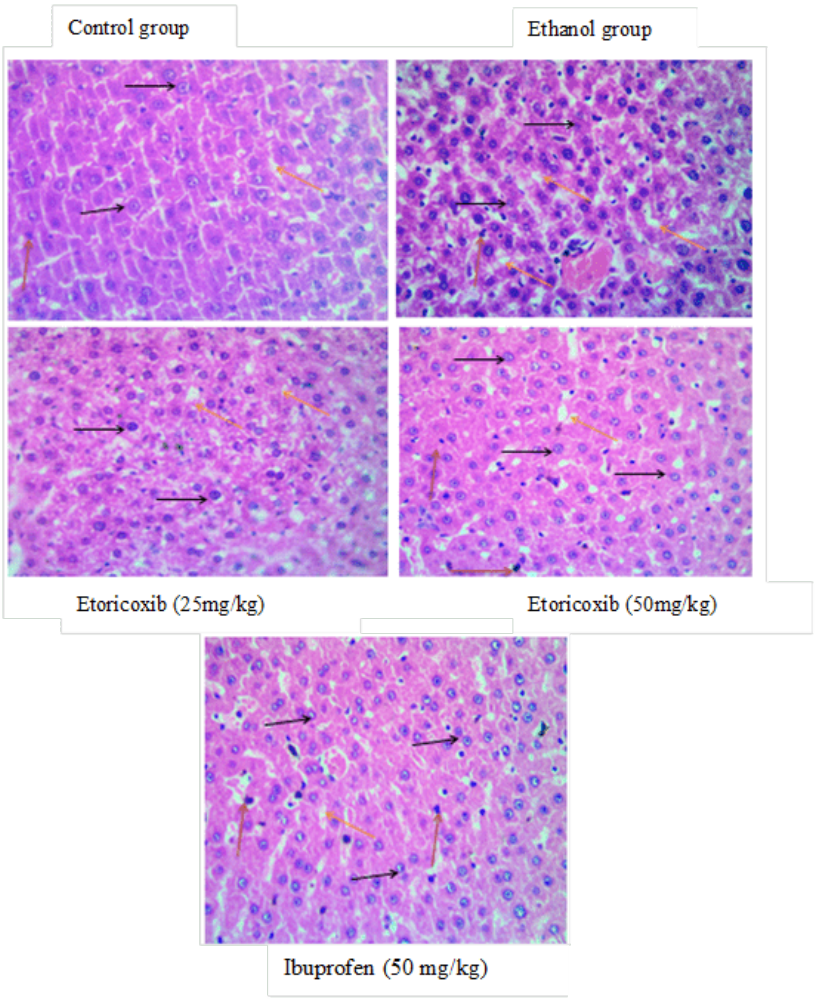

FIGURE 4.12: Hematoxylin and eosin staining of cross-sectional liver tissue across experimental

(50 mg/kg) significantly protected the liver against ethanol-induced injury which shows recovery of hepatocytes .

Chapter 5

Discussion

Alcohol-related liver disease (ALD) encompasses a range of liver conditions that are caused by excessive and prolonged alcohol consumption. In the current study, etoricoxib was evaluated for hepatoprotective activity against ethanol induced liver damage in mice. Molecular docking, liver function tests, cytokines levels, histophathology were done to assess hepatoprotective effect of etoricoxib. The hepatic microsomal ethanol oxidizing system's major enzyme, CYP2E1, is crucial for the metabolism of ethanol. Ethanol consumption promotes CYP2E1 activity, increasing the generation of ROS. Ethanol considerably enhanced ALT and AST levels in the liver. ALD is also associated with increased TNF-α, all of which contribute to hepatocyte dysfunction. This study intended to evaluate the hepatoprotective and anti-inflammatory abilities of etoricoxib, a selective COX-2 inhibitor, in a mice model of ethanol-induced hepatotoxicity. We sought to determine the effectiveness of etoricoxib (25 mg/kg) as low dose and (50 mg/kg) high dose) in comparison to non-selective anti-inflammatory drug, ibuprofen (50 mg/kg), based on the molecular docking, main biochemical investigation parameters ALT/AST, total protein (BCA assays), and pro-inflammatory cytokines TNF-α Sample ELISA kits, H&E staining. In the present study, ethanol administration (20% v/v) (5 g/kg) induced a significant increase in both ALT (170 ± 5.0 U/L) and AST (127 ± 4.0 U/L) compared to the control group (ALT: 45 ± 2.5 U/L; AST: 32 ± 2.0 U/L). These findings align with previous reports demonstrating that chronic ethanol exposure promotes

oxidative stress, mitochondrial dysfunction, and hepatocyte necrosis, leading to transaminase leakage.

Treatment with etoricoxib ((25 mg/kg) and (50 mg/kg)) and ibuprofen (50 mg/kg) significantly attenuated ethanol-induced elevations in ALT and AST.

Etoricoxib (50 mg/kg) exhibited the strongest hepatoprotective effect, reducing ALT to 60 ± 2.1 U/L and AST to 45 ± 3.2 U/L, closely approximating control levels. Etoricoxib (25 mg/kg) showed moderate protection (ALT: 130 ± 2.8 U/L; AST: 90 ± 1.9 U/L).

Ibuprofen (50 mg/kg) also reduced transaminases (ALT: 75 ± 3.5 U/L; AST: 57 ± 3.0 U/L) but was less effective than high-dose etoricoxib. These results suggest a dose-dependent hepatoprotective effect of etoricoxib, consistent with prior studies demonstrating that selective COX-2 inhibitors mitigate liver injury by reducing inflammatory prostaglandinns (PGE2) and oxidative stress.

These finding consistent with the previous work that showed, etoricoxib decreased oxidative stress and liver fibrosis in a CCl_4-induced liver injury model.

In our study , etoricoxib at a dose of (50 mg/kg) reduced ALT to 48%, similar to the finding of Zakiyah et al. (2022) which reported a 45% decrease in ALT for a CCl_4-induced hepatotoxicity model. TNF-α levels were decreased by 36% in our model, which lies just below the results of Malik et al. (2023) which found a 35% reduction utilizing COX-2 inhibitors in alcoholic liver disease.

Etoricoxib better effect can be explained by the selective inhibition of COX-2 causing a decrease in related PGE2-induced inflammation, retaining COX-1, and thus retaining gastrointestinal integrity an advantage to non-selective NSAIDs such as ibuprofen. The BCA assay measured the overall protein content present in liver tissue lysates. This assay was able to provide some insight into the amount of protein lost due to degradation and the impaired synthetic capacity of the liver tissue during a state of inflammatory stress. The ethanol-only group exhibited protein concentration consistent with damaged hepatocyte functional capacity with respect to synthetic capacity and acute liver injury.

When comparing the treatment groups to the control tissues, the etoricoxib blocks the amount of degraded protein according to the BCA assay and provide an overall protein amount that was closer to the baseline than they were in the ethanol-only group tissues.

Etoricoxib treatment groups displayed reconciled protein levels that are approaching baseline. The maintenance of hepatic architecture and function indicated that etoricoxib also preserved overall liver function as well suggested that functional proteins can be lost during a state of hepatocellular injury due to oxidative damage and cytoskeletal disintegration.

TNF-α is a well-known pro-inflammatory cytokine which can be involved in the pathogenesis of ethanol-induced liver injury. Ethanol tissues exhibited a significant increase in TNF-α concentrations in hepatic tissue when compared to baseline levels with regards to the tissue.

The increased TNF-α production can be explained by the use of oxidative stress due to ethanol metabolism and subsequent NF-κB activation of TLR-4 signaling in the lipopolysaccharide induced activation of Kupffer cells. Etoricoxib (50 mg/kg) significantly reduced the TNF-α expression in a dose-dependent manner with greater efficacy of TNF-α suppression when compared to ibuprofen.

Comparisons to Literature, our findings support the potential therapeutic role of etoricoxib over ibuprofen for ethanol-induced liver damage. Ibuprofen inhibits COX-1 and COX-2 by contrast selective COX-2 inhibition by etoricoxib preferentially reduces pro-inflammatory prostaglandins without negatively affecting protective prostanoids and minimizes gastrointestinal mucosal injury.

There is also preclinical evidence from Shen et al. (2011) and Shortall et al. (2021) that includes suggestions that etoricoxib has anti-fibrotic, and anti-oxidative effects, which we were able to see through our results as indicated by improved ALT, AST, and TNF-α.

Engelmann et al. 2025 emphasized the co-therapeutic roles of TNF-α and IL-6 in ethanol-mediated hepatic inflammation paving the way to both being hypothetically

as therapeutic agent in infectious settings. Mechanistic understanding COX-2, NF-κB, and Hepatic Inflammation, COX-2, NF-κB pathway, as it is implicated in ethanol-induced liver injury, is significant.

Ethanol exposure generates ROS, which activates NF-κB via an IκB-mediated degradation pathway thereby promoting the transcriptional initiation of TNF-α, and pro-inflammatory agents. Through the inhibition of COX-2, etoricoxib inhibits PGE2 synthesis, and indirectly prevents NF-κB activation.

Upon examining our etoricoxib treated groups, demonstrated decrease of TNF-α, substantiates this pathway as a mechanistic target for possible therapeutically intervention. The current study represents systematically investigated the hepato-protective and anti-inflammatory effects of etoricoxib, a selective COX-2 inhibitor, in mice model of ethanol induced hepatotoxicity.

Biochemical markers, such as ALT and AST, total protein content via BCA assay and the pro-inflammatory cytokine TNF-α via ELISA, this study provides substantial evidence to support the therapeutic potential of etoricoxib in attenuating ethanol-induced liver injury.

Ethanol (20% v/v) (5 g/kg) exposure resulted in a well-defined hepatocellular injury manifested by elevated serum transaminases and elevated TNF-α, discovering the hallmark applicability of oxidative stress and inflammation consistent with alcoholic liver disease (ALD). Etoricoxib (50 mg/kg) resulting in the greatest hepatoprotective and anti-inflammatory effect, shown by the magnitude of change in ALT, AST and TNF-α.

Comparison to the standard reference drug ibuprofen non-selective COX inhibitor showed that etoricoxib produced a greater hepatoprotective effect, which likely results from its selective COX-2 inhibition and subsequent down regulation of the pro-inflammatory prostaglandin E2 (PGE2) without negatively impacting the cytoprotective effects of COX-1.

These findings emphasized the mechanistic advantage of etoricoxib in maintaining hepatic integrity while reducing off-target toxicity. This study demonstrates

the importance of the COX-2/PGE2/NF-κB signaling axis in ethanol-induced liver inflammation.

Additionally, the data presented etoricoxib as a potential pharmacological target and inhibitor of the COX-2/NF-kB inflammatory pathway. The observed efficacy in a dose-dependent relationship suggests that greater precision is required when titrating etoricoxib, as greater doses appear to augment protective effects. It is equally important to acknowledge the scope and limitations of this study.

The immunologic and biochemical data provided compelling evidence of the efficacy of etoricoxib for ameliorating hepatic insult. This study adds to the growing line of research showing selective COX-2 inhibition may be a viable and superior means to manage ethanol induced liver inflammation.

All the molecular docking data showed that etoricoxib has a strong binding affinity towards COX-2 which has been documented extensively and the important pro-inflammatory cytokines TNF-α and NF-κB. The TNF-α binding was the most intriguing because it provides an opportunity to modulate cytokine mediated signaling pathways, in addition to COX-2 inhibition. TNF-α is a central mediator in chronic inflammation, and it stimulates downstream transcription factors like NF-κB.

The binding score of NF-κB was lower than TNF-α, the interaction with NF-κB was still there and indicates a potential regulatory effect as well. The results provide further support of the hypothesis that etoricoxib may exhibit additional anti-inflammatory activity through diminished overall levels of cytokine activity. This phenomenon may compliment etoricoxib clinical effectiveness for chronic diseases associated with increased cytokine expression, such as rheumatoid arthritis and other autoimmune diseases.

In comparison with etoricoxib, ibuprofen did show some capacity to bind to cytokines TNF-α and NF-κB, but with lower binding affinities than etoricoxib. Ibuprofen forms stable construct with their targets, but this suggests its binding is less specific and therefore potentially less effective for direct modulation of cytokine-mediated inflammation.

As a non-selective NSAID, ibuprofen's more general and weaker binding behavior would be consistent with its typical pharmacodynamics profile. The moderate TNF-α binding indicates that ibuprofen has some potential to contribute to cytokine suppression and may partially relieve inflammation in an acute inflammatory state.

The weak binding to NF-κB suggests minimal impact on downstream gene regulatory pathways while etoricoxib would have a greater impact. The data maybe suggest though ibuprofen is able to bind cytokine targets, the bulk of its anti-inflammatory action is likely still primarily through COX inhibition and not through modulation of cytokines. The weak binding to NF-κB suggests minimal impact on downstream gene regulatory pathways while etoricoxib would have a greater impact. This data has suggested that the ibuprofen is able to bind cytokine targets, the bulk of its anti-inflammatory action is likely still primarily through COX inhibition and not through modulation of cytokines.

Molecular docking is an important in silico technique used in drug discovery to explore the interaction at the atomic level between small molecules and target macromolecules. In this study, molecular docking established the binding affinity of etoricoxib and ibuprofen against inflammation-associated proteins, COX-2, TNF-α, and NF-κB. Evidently, etoricoxib showed the highest binding affinity towards the target COX-2 (-8.9 kcal/mol) followed by TNF-α (-8.3 kcal/mol) and NF-κB (-6.3 kcal/mol).

This shows that etoricoxib has a good stable interaction through various inflammatory pathways. Careful three-dimensional (3D) and two-dimensional (2D) molecular interaction presentations showed that all three of the small molecules successfully fit within the active pockets of the enzyme. With COX-2 protein binding it supplemented etoricoxib as a hydrogen bonding interaction with Arg120 and Tyr355 alongside hydrophobic contacts with Val349 and Leu352, which are consistent with the known COX-2 inhibition profile. The binding of etoricoxib to TNF-α purported interactions with Leu57 and Tyr119, while NF-κB was partially driven contact by van der Waals forces. The results of molecular modelling are congruent with previous literature that supports such interactions, to described binding modalities to similar COX-2 binding configurations with etoricoxib.

In terms of docking scores (COX-2: -7.0 kcal/mol, TNF-α: -6.9 kcal/mol, NF-κB: -5.4 kcal/mol), ibuprofen has relatively lower binding energies suggesting less preferred interactions. Similar to the above findings, the interactions of ibuprofen were not shown to have the specific stabilizing hydrogen bonds as shown with etoricoxib, which exemplifies the pharmacologic differences between selective and non-selective NSAIDs.

Research suggested, COX-2 selective inhibitors out perform traditional NSAIDs in suppressing targeted cytokines. The moderate TNF-α binding may imply some potential in terms of anti-inflammatory activity of ibuprofen, however, the limited findings with NF-κB may not suggest broader anti-inflammatory activity. Molecular docking provides not only confirmation with the biochemical data, but further understanding of the mechanistic action of etoricoxib as a multi-target agent engagement with COX-2, TNF-α, and NF-κB pathways leads to superior anti-inflammatory potential.

Histological evaluation using hematoxylin and eosin (H&E) staining is still an important diagnostic tool for detecting changes in liver structure. In this study, liver sections from ethanol-treated mice demonstrate the classic markers of liver injury, including hepatocellular ballooning, loss of sinusoidal spaces, necrosis, and lymphocytic infiltration. These findings substantiate the previously identified histopathological changes seen in ALD. Etoricoxib treatment at both (25 mg/kg) and (50 mg/kg) offered a substantial restoration of liver architecture. The results showed preserved sinusoidal spacing, reduction in inflammatory infiltrates, and minimal hepatocyte necrosis.

Those findings parallel the compound's biochemical and molecular profiles, and reinforce its hepatoprotective potential. The hepatoprotective effect of etoricoxib was much greater than ibuprofen, which showed only partial restoration of liver tissue structure. This is consistent with ibuprofen's less selective mechanism. This finding complements a comparative histological study in which selective COX-2 inhibitors diminished ethanol-induced liver inflammation greater than that of non-steroidal anti-inflammatory drugs.

In addition, the histopathological findings in etoricoxib-treated groups demonstrate its proposed mechanism of action involving the downregulation of COX-2 and TNF-α, limiting immune cell infiltration, and necrotic signaling cascade. Overall, H&E staining provides evidence of pharmacological activity with etoricoxib on the hepatic structure and function and lends further morphological evidence that supports the molecular and biochemical evidence presented in this study. This is the first research to evaluated etoricoxib's hepatoprotective potential in ethanol-induced hepatotoxicity models. It incorporated both biochemical and molecular docking studies which contributed multi-dimensional evidence. The two different doses used allows for an assessment of dose-dependent efficacy.

5.1 Limitations

This study provides clear evidence for the hepatoprotective and anti-inflammatory potential of etoricoxib in an ethanol induced hepatotoxicity model, there are some aspects that limit the ability to interpret and translate findings. The acute ethanol orientation of this study, while effective in eliciting hepatic injury and inflammatory responses, does not confidently emulate the complicated and chronic progression of alcohol related liver disease in humans, such as the prolonged oxidative stress, fibrotic processes, and development of cirrhosis. The pharmacokinetics of etoricoxib in hepatic tissue, which contributes to our understanding of the metabolism, distribution and hepatic clearance profile, is not identified in this study, making it difficult to transpose these dose-response relationships into clinical conditions. Advanced histopathological grading was not utilized in this study and the key markers of TGF- β, MDA and GSH were not evaluated. This does not provide the researcher much insight into the fibrotic change and oxidative status of the liver. Although our findings suggest there was strong hepatoprotection, the lack of gene expression assays (i.e. COX-2, NF-κB mRNAs levels) limits our ability to provide mechanistic confirmation. Overall, these factors highlight the need for more prolonged studies utilizing chronic ethanol exposure, acknowledge the differences observed in male and female cohorts, and explore biomarkers that allow for a more complete understanding of the hepatic injury.

Chapter 6

Conclusion and Future Work

The current study was performed in an order to provide a comprehensive evaluation of the hepatoprotective and anti-inflammatory effect of etoricoxib, a selective COX-2 inhibitor, in an established mice model of ethanol-induced hepatotoxicity. Chronic ethanol use is a global public health problem and leads to hepatic injuries ranging from fatty liver, hepatitis and cirrhosis as a result in cumulative oxidative stress, mitochondrial dysfunction and prolonged inflammatory responses. The study aimed to assess whether etoricoxib, through selective inhibition of COX-2, could attenuate biochemical and inflammatory responses, highlighting its potential as a pharmacological intervention.

The results of this study provide strong experimental evidence supporting the hepatoprotective potential of etoricoxib in the setting of ethanol-induced liver injury. Administration of ethanol caused substantial liver injury in mice, as demonstrated by a significant increase in serum liver enzymes ALT and AST, increased levels of TNF-α the pro-inflammatory cytokine, and increased hepatic protein content determined by BCA protein assay. These findings indicate compromised hepatocyte integrity, oxidative stress, and continuing inflammation, which are key pathological features of ethanol-induced hepatotoxicity. Etoricoxib, selectively inhibits COX-2, exhibited a dose-dependent protective effect in the ethanol-induced liver injury model. Mice administered (50 mg/kg) of etoricoxib reduced ALT and AST levels compared to ethanol-only group and levels were similar to the control group.

The etoricoxib (50 mg/kg) treatment ALT and AST showed significant hepatoprotective effects, by down-regulating inflammatory signaling and limiting hepatocyte damage caused by oxidative stress.

Etoricoxib (25 mg/kg) treatment did improve ALT and AST markers, but to a lesser extent, suggesting that (50 mg/kg) etoricoxib conferred a greater therapeutic benefit than (25 mg/kg).

The reducing levels of TNF-α by etoricoxib is of particular importance, as TNF-α is the major cytokine involved in the disease process of alcoholic liver disease. In addition, inhibition of TNF-α expression by etoricoxib likely interrupted the pro-inflammatory signaling cascade activated by NF-κB, thus blocking both apoptosis in hepatocytes or neutrophil infiltration into injured liver tissue.

These results are consistent with other literature reporting, COX-2 inhibition with the down-regulation of cytokine activity and better liver outcomes. The BCA assay protein concentration was lower in the etoricoxib treated groups, indicating some level of protection of hepatocyte function and an attenuation of cellular stress.

In comparison to ibuprofen (50 mg/kg) standard reference drug, treatment did lead to hepatoprotective effects but less than etoricoxib (50 mg/kg).

This is primarily due to Ibuprofen's non-selective inhibition of both COX-1 and COX-2, which would lead to compromised gastro-intestinal and renal protective pathways. In contrast, etoricoxib's selective COX-2 inhibition would adequately manage inflammation, while preserving the synthesis of homeostatic prostaglandins regulated by COX-1, thus providing a better safety and efficacy profile. The study findings further support the view that COX-2 targeting can be a tactical method to manage ethanol-induced hepatic injuries.

This figure compares the hepatoprotective mechanisms of Etoricoxib and Ibuprofen in ethanol-induced liver injury. Etoricoxib selectively inhibits COX-2, reducing inflammation and oxidative stress more effectively. Both drugs improve liver biomarkers and histology, but Etoricoxib shows a more targeted anti-inflammatory profile.

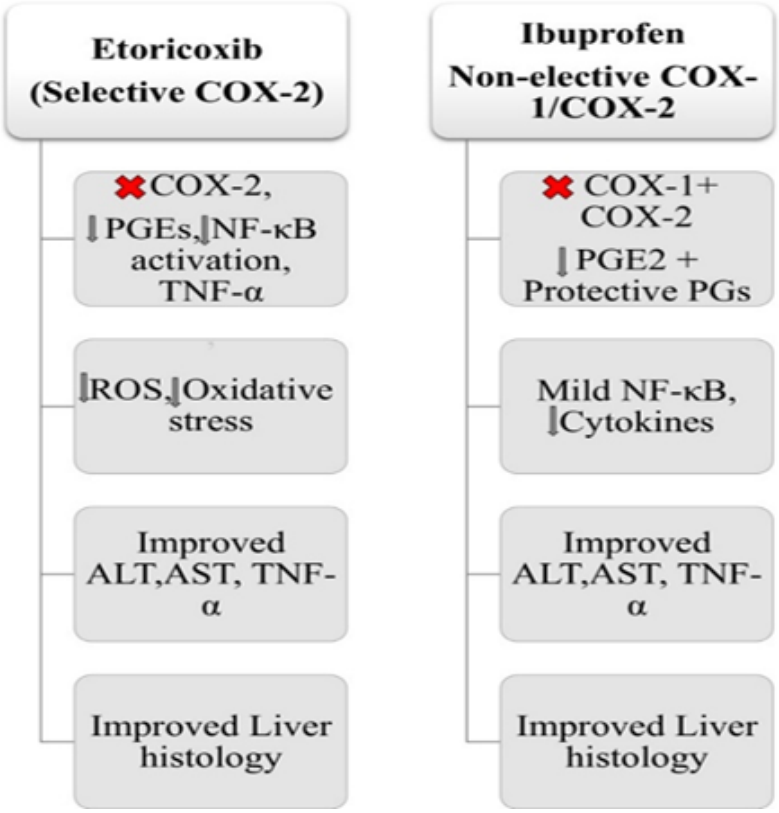

FIGURE 6.1: Comparative mechanistic overview of Etoricoxib and Ibuprofen in ethanol-induced hepatotoxicity.

Molecular docking analysis provided additional evidence that etoricoxib has a strong capacity to bind to active sites of COX-2, TNF-α, and NF-κB, supporting its multifactorial therapeutic mechanism. The combination of these actions contributed to both the down-regulation of pro-inflammatory mediators and the protection of hepatic architecture. The histopathological aspect provided by H&E staining adds valuable perspective to the level of liver damage and the protective treatment response in ethanol-induced hepatotoxicity. The sections of liver tissue from the ethanol treatment group displayed significant histological alterations including extensive hepatocellular necrosis, infiltration of inflammatory cells, marked cytoplasmic vacuolation, and loss of normal hepatic architecture, which area characteristic of alcohol-induced liver damage. The regimens involving etoricoxib treatment allowed for a considerable restoration of hepatic histoarchitecture, reduction of necrotic foci and decreased inflammatory cell infiltrates, with the optimum response in the (50 mg/kg) dose group, presumably indicating hepatoprotection in some capacity. Partial improvement was observed in the ibuprofen group, but less effective

than etoricoxib high-dose. Overall, these findings corroborate the histological presentation from this study, which shows that etoricoxib was able to confer structural protection under intoxication with ethanol-induced liver injury potentially via COX-2 selectivity and anti-inflammatory pathways, and also extended to levels of restoration of normal hepatic architecture. Consistent with the findings from the biochemical and cytokine results, the H&E staining confirmed the protective effects of etoricoxib at the tissue level.

This study indicated that etoricoxib has a substantial protective effect against alcohol-induced liver injury, demonstrated by robust findings in a mice model. Administration of etoricoxib was integral in preventing an increases in serum ALT, AST and levels of TNF-α. Etoricoxib administration assisted in restoration of protein homeostasis in the liver. The high-dose etoricoxib (50 mg/kg) resulted in significantly better outcomes than both low-dose etoricoxib, and ibuprofen, thereby offering a potentially safer and more directed pharmacologic approach to alcohol-related liver disease. These data provide an important rationale for etoricoxib as a useful pharmacological option in the context of alcohol-related liver injury.

6.1 Future Prospective

The favorable outcomes of the present study indicate that etoricoxib a selective COX-2 inhibitor markedly diminished hepatic inflammation and injury markers ALT, AST, and TNF-α. The data collected in this pilot study will serve as a basis to be further explored in pharmacodynamics and pharmacokinetic studies, and subsequent studies should focus on dose-optimization studies that can be explored further in larger animal models utilizing time-dependent pharmacological profiles. A more robust role of etoricoxib could also be identified using additional bioanalytical techniques such as LC-MS/MS, to better characterize the systemic (exposed to the blood) and hepatic concentration-time profile of etoricoxib and active metabolites. Given the marked anti-inflammatory effects of etoricoxib, it would be prudent to also inquire about its molecular targets outside of COX-2 such as NF-kB signaling

and the inflammasome pathways activated in ethanol-mediated liver injury. Further studies could utilize gene profiling, transcriptomics and proteomics to further appreciate downstream regulatory networks induced by treatment with etoricoxib.

Molecular docking in this dissertation scope demonstrated positive interactions of etoricoxib with COX-2, TNF-α, and NF-κB, reinforcing the multi-target approach. While achieving these goals, subsequent computational simulations, (molecular dynamics (MD) simulations and calculating binding free energy (MM/PBSA or MM/GBSA), can be done to affirm the stability of ligand-receptor complexes under physiological conditions. Utilizing structure-based drug design (SBDD) approaches one can potentially generate and evaluate analogues of etoricoxib that demonstrate a higher specificity, improved safety margins, and no off-target effects compared with ibuprofen. Following this approach, etoricoxib derivatives can be evaluated via high-throughput screening resulting in development of novel COX-2 selective therapeutics that have improved hepatic bioavailability and longer half-lives.

The clinical importance of these analogues may include a stronger potential for limiting chronic inflammation, independently of ethanol, and loosely limiting the cardiovascular risks associated with the cumulative consequences of COX-2 inhibition. We modeled acute hepatoxicity from ethanol, in the clinical realm, individuals often present with chronic exposure more closely resembling alcoholic steatohepatitis, fibrosis, and cirrhosis. Future research should implement chronic exposure models up to 4-12 weeks in order to best mimic human pathophysiology. Due to the substantial hepatoprotective effect seen throughout the dose levels, longitudinal studies should also evaluate combination therapy with NAC (both NAC, and COX-2 inhibition) in an attempt to maximize antioxidant protection in conjunction with COX-2 inhibition. Utilize molecular studies evaluating caspase-3 and Bcl-2 expression to elaborate on the anti-apoptotic mechanism of etoricoxib's protective effects.

Chronic exposure with these models would allow all histopathological parameters such as degree of steatosis, lobular inflammation, and fibrosis scores (e.g. METAVIR index or NAFLD Activity Score). Analysis of histopathology following long-term etoricoxib treatment can determine. If etoricoxib induces effects associated with structure or regeneration primarily on the hepatic stellate cells, deposition of the

extracellular matrix, and angiogenesis. Investigating longer etoricoxib treatment may also provide insight on whether it can induce antifibrotic effects, potentially representing a treatment approach for later-stage alcoholic liver disease or non-alcoholic fatty liver. Oxidative stress is one of the essential pathogenic mechanisms for ethanol-induced hepatotoxicity by lipid peroxidation, but also through ROS-mediated mitochondrial dysfunction and damage.

Future studies might look further into combination therapies with etoricoxib that include antioxidants such as N-acetylcysteine, silymarin or resveratrol to improve the hepatoprotective ability of etoricoxib. The combination of these agents may provide added protective effects by dual inhibition of the inflammatory and oxidative stress pathways and subsequent tissue damage.

Another alternative, along with combination therapy, is nanocarrier(s) drug delivery systems that may provide more first-pass hepatic targeting and therapeutic efficacy for etoricoxib. Nano-formulations including liposomes, polymeric nanoparticles, or solid lipid nanoparticles could improve the bioavailability of etoricoxib, reduce systemic toxicity, and provide slow release. For instance, liver-specific delivery using galactose-modified nanoparticles may improve the accumulation of etoricoxib in hepatocytes and Kupffer cells. Moving the preclinical findings to clinical implementation requires identification of reliable biomarkers.

In additional work, larger biomarker panels using not only ALT, AST, and TNF-α, but also IL-1β, IL-6, TGF-β, α-SMA, and caspase-3, could be examined using multiplex ELISA or transcriptomic profiling. Pharmacodynamics analysis of how etoricoxib impacts these biomarkers would help to determine predictive markers of drug efficacy and safety. Clinical trials in patients with early-stage alcoholic liver disease could evaluate etoricoxib hepatoprotective role under rigorously controlled dosing and monitoring. Important clinical endpoints could include normalization of serum transaminases as well as histologic improvement, reduction in inflammatory cytokines, and quality-of-life measures.

The clinical trial could be modelled as a Phase I/II study design, with the Phase I evaluation of patients with mild-to-moderate steatohepatitis, before progressing

to patients with fibrosis and cirrhosis. The results indicated that etoricoxib performed better than ibuprofen. Nevertheless, further comparisons with other COX-2 inhibitors such as (celecoxib and rofecoxib) and hepatoprotective agents (such as silymarin and ursodeoxycholic acid) will allow the current study to be placed into a wider therapeutic context.

In addition, monitoring etoricoxib's cardiovascular and renal adverse effects in longer-term studies will help detect potential adverse events associated with COX-2 inhibition. It will be necessary in any future studies to consider hepatoprotection versus systemic safety. Examining organ type specific toxicity, cardiac and renal oxidative load, and blood pressure effects in treated animal studies may address this issue. Pharmacogenetic screening could also provide insight into inter-individual differences in metabolism of drugs and risk of adverse effects.

Bibliography

[1] I. Ogobuiro *et al.*, "Physiology, gastrointestinal," in *StatPearls* [Online]. StatPearls Publishing, 2023. [Online]. Available: https://www.ncbi.nlm.nih.gov/books/NBK537103/

[2] V. Mahadevan, "Anatomy of the liver," *Surgery (Oxford)*, vol. 38, no. 8, pp. 427–431, 2020.

[3] H. K. Mohajan, "A study on functions of liver to sustain a healthy liver," *Innov. Sci. Technol.*, vol. 4, no. 1, pp. 77–87, 2025.

[4] O. F. Abdullah, D. A. Jasim, and Q. S. Atwan, "Biochemical and total antioxidant effects of iron oxide nanoparticles on liver mice," 2025.

[5] R. Manco and S. Itzkovitz, "Liver zonation," *J. Hepatol.*, vol. 74, no. 2, pp. 466–468, 2021.

[6] R. Wang *et al.*, "Gut microbiome, liver immunology, and liver diseases," *Cell. Mol. Immunol.*, vol. 18, no. 1, pp. 4–17, 2021.

[7] M. Mihajlovic and M. Vinken, "Mitochondria as the target of hepatotoxicity and drug-induced liver injury: Molecular mechanisms and detection methods," *Int. J. Mol. Sci.*, vol. 23, no. 6, p. 3315, 2022.

[8] P. G. Thomes *et al.*, "Natural recovery by the liver and other organs after chronic alcohol use," *Alcohol Res.: Current Rev.*, vol. 41, no. 1, p. 05, 2021.

[9] S. M. Woo *et al.*, "Highlights of the drug-induced liver injury literature for 2021," *Expert Rev. Gastroenterol. Hepatol.*, vol. 16, no. 8, pp. 767–785, 2022.

[10] M. M. Bani *et al.*, "Photonic crystal fiber sensors in the THz domain: A leap forward in alcohol detection," *Heliyon*, vol. 10, no. 24, 2024.

[11] A. U. Atumeyi, T. T. Ligom, and J. T. Tivkaa, "Intake and abuse of psychoactive substances and its relative consequences: A review," *Sci. J. Anal. Chem.*, vol. 9, no. 2, pp. 39–49, 2021.

[12] S. H. Park and D. J. Kim, "Global and regional impacts of alcohol use on public health: Emphasis on alcohol policies," *Clin. Mol. Hepatol.*, vol. 26, no. 4, p. 652, 2020.

[13] G. Ayares *et al.*, "Public health measures and prevention of alcohol-associated liver disease," *J. Clin. Exp. Hepatol.*, vol. 12, no. 6, pp. 1480–1491, 2022.

[14] M. Abudayyak and T. Boran, "Is UR-144 synthetic cannabinoid toxic to the neuronal cells: An in vitro evaluation," *Fabad Eczacılık Bilimler Dergisi*, vol. 50, no. 1, pp. 39–50, 2025.

[15] P.-H. Chen, "Investigations across the care continuum for alcohol-associated liver disease," Ph.D. dissertation, Johns Hopkins Univ., Baltimore, MD, USA, 2023.

[16] E. R. Chalhoub and J. M. Belovich, "Quantitative analysis of the interaction of ethanol metabolism with gluconeogenesis and fatty acid oxidation in the perfused liver of fasted rats," *Arch. Biochem. Biophys.*, vol. 718, p. 109148, 2022.

[17] M. Chen, W. Zhong, and W. Xu, "Alcohol and the mechanisms of liver disease," *J. Gastroenterol. Hepatol.*, vol. 38, no. 8, pp. 1233–1240, 2023.

[18] H. K. Seitz *et al.*, "Alcoholic liver disease," *Nat. Rev. Dis. Primers*, vol. 4, no. 1, p. 16, 2018.

[19] G. G. M. Scarlata *et al.*, "The role of cytokines in the pathogenesis and treatment of alcoholic liver disease," *Diseases*, vol. 12, no. 4, p. 69, 2024.

[20] L.-Z. Kong *et al.*, "Pathogenesis, early diagnosis, and therapeutic management of alcoholic liver disease," *Int. J. Mol. Sci.*, vol. 20, no. 11, p. 2712, 2019.

[21] R. Adhikari *et al.*, "Spermidine prevents ethanol and lipopolysaccharide-induced hepatic injury in mice," *Molecules*, vol. 26, no. 6, p. 1786, 2021.

[22] P. Ginès *et al.*, "Liver cirrhosis," *Lancet*, vol. 398, no. 10308, pp. 1359–1376, 2021.

[23] C. Engelmann, I. W. Zhang, and J. Clària, "Mechanisms of immunity in acutely decompensated cirrhosis and acute-on-chronic liver failure," *Liver Int.*, vol. 45, no. 3, p. e15644, 2025.

[24] A. Sadighi, L. Leggio, and F. Akhlaghi, "Development of a physiologically based pharmacokinetic model for prediction of ethanol concentration-time profile in different organs," *Alcohol Alcohol.*, vol. 56, no. 4, pp. 401–414, 2021.

[25] M. Akande *et al.*, "The impacts of L-arginine on biochemical parameters and oxidative stress in rats exposed to subacute imidacloprid toxicity," 2023.

[26] L. Di *et al.*, "The role of alcohol dehydrogenase in drug metabolism: Beyond ethanol oxidation," *AAPS J.*, vol. 23, no. 1, p. 20, 2021.

[27] U. Gyaneshwari *et al.*, "Alcohol dehydrogenase: Structural and functional diversity," in *Integrative Approaches to Biotechnology*. CRC Press, 2023, pp. 249–265.

[28] M. L. Contreras-Zentella, D. Villalobos-García, and R. Hernández-Muñoz, "Ethanol metabolism in the liver, the induction of oxidant stress, and the antioxidant defense system," *Antioxidants*, vol. 11, no. 7, p. 1258, 2022.

[29] R. Teschke *et al.*, "Alcoholic liver disease and the co-triggering role of MEOS with its CYP 2 E 1 catalytic cycle and ROS," *Arch. Gastroenterol. Res.*, vol. 2, no. 1, pp. 9–25, 2021.

[30] K. Shortall *et al.*, "Insights into aldehyde dehydrogenase enzymes: A structural perspective," *Front. Mol. Biosci.*, vol. 8, p. 659550, 2021.

[31] Y. Jiang *et al.*, "Alcohol metabolizing enzymes, microsomal ethanol oxidizing system, cytochrome P450 2E1, catalase, and aldehyde dehydrogenase in alcohol-associated liver disease," *Biomedicines*, vol. 8, no. 3, p. 50, 2020.

[32] N. S. Marinkovic, M. Li, and R. R. Adzic, "Pt-based catalysts for electrochemical oxidation of ethanol," *Electrocatalysis*, pp. 1–39, 2020.

[33] Q. Wang *et al.*, "A novel bifunctional aldehyde/alcohol dehydrogenase catalyzing reduction of acetyl-CoA to ethanol at temperatures up to 95 °C," *Sci. Rep.*, vol. 11, no. 1, p. 1050, 2021.

[34] Y. M. Yang, Y. E. Cho, and S. Hwang, "Crosstalk between oxidative stress and inflammatory liver injury in the pathogenesis of alcoholic liver disease," *Int. J. Mol. Sci.*, vol. 23, no. 2, p. 774, 2022.

[35] O.-J. Sul and S. W. Ra, "Quercetin prevents LPS-induced oxidative stress and inflammation by modulating NOX2/ROS/NF-kB in lung epithelial cells," *Molecules*, vol. 26, no. 22, p. 6949, 2021.

[36] L. D. Nelin *et al.*, "Cyclooxygenase-2 deficiency attenuates lipopolysaccharide-induced inflammation, apoptosis, and acute lung injury in adult mice," *Amer. J. Physiol.-Regul. Integr. Comp. Physiol.*, vol. 322, no. 2, pp. R126–R135, 2022.

[37] X. Norel *et al.*, "International union of basic and clinical pharmacology: Differences and similarities between human and rodents concerning prostaglandin EP1-4 and IP receptors: Specific roles in pathophysiologic conditions," *Pharmacol. Rev.*, 2020.

[38] J. Shah and R. Kotadiya, "A critical review on analytical methods for recently approved FDC drugs: Pregabalin and etoricoxib," *Crit. Rev. Anal. Chem.*, vol. 52, no. 5, pp. 1048–1068, 2022.

[39] L. Franco-de la Torre *et al.*, "Analgesic efficacy of etoricoxib following third molar surgery: A meta-analysis," *Behav. Neurol.*, vol. 2021, no. 1, p. 9536054, 2021.

[40] L. L. Mazaleuskaya *et al.*, "PharmGKB summary: Ibuprofen pathways," *Pharmacogenet. Genomics*, vol. 25, no. 2, pp. 96–106, 2015.

[41] Y. A. Nartey *et al.*, "Mortality burden due to liver cirrhosis and hepatocellular carcinoma in Ghana: Prevalence of risk factors and predictors of poor in-hospital survival," *PLoS One*, vol. 17, no. 9, p. e0274544, 2022.

[42] C. Wang *et al.*, "Neuropathic injury-induced plasticity of GABAergic system in peripheral sensory ganglia," *Front. Pharmacol.*, vol. 12, p. 702218, 2021.

[43] D. Patel *et al.*, "Synbiotic intervention ameliorates oxidative stress and gut permeability in an in vitro and in vivo model of ethanol-induced intestinal dysbiosis," *Biomedicines*, vol. 10, no. 12, p. 3285, 2022.

[44] P. K. Shukla *et al.*, "Chronic stress and corticosterone exacerbate alcohol-induced tissue injury in the gut-liver-brain axis," *Sci. Rep.*, vol. 11, no. 1, p. 826, 2021.

[45] J. George *et al.*, "Cellular and molecular mechanisms of hepatic ischemia-reperfusion injury: The role of oxidative stress and therapeutic approaches," *Redox Biol.*, p. 103258, 2024.

[46] K.-K. Abassa *et al.*, "Effect of alcohol on clinical complications of hepatitis virus-induced liver cirrhosis," *BMC Gastroenterol.*, vol. 22, no. 1, p. 130, 2022.

[47] T. Ren *et al.*, "Hepatic injury and inflammation alter ethanol metabolism and drinking behavior," *Food Chem. Toxicol.*, vol. 136, p. 111070, 2020.

[48] G. Kubiak-Tomaszewska *et al.*, "Molecular mechanisms of ethanol biotransformation: Enzymes of oxidative and nonoxidative metabolic pathways in human," *Xenobiotica*, vol. 50, no. 10, pp. 1180–1201, 2020.

[49] M. Mackus *et al.*, "Alcohol hangover versus dehydration revisited: The effect of drinking water to prevent or alleviate the alcohol hangover," *Alcohol*, 2024.

[50] M. Comporti *et al.*, "Ethanol-induced oxidative stress: Basic knowledge," *Genes Nutr.*, vol. 5, pp. 101–109, 2010.

[51] C. Yan *et al.*, "Pathogenic mechanisms and regulatory factors involved in alcoholic liver disease," *J. Transl. Med.*, vol. 21, no. 1, p. 300, 2023.

[52] Z. Zhang *et al.*, "Reactive oxygen species as key molecules in the pathogenesis of alcoholic fatty liver disease and nonalcoholic fatty liver disease: Future perspectives," *Curr. Issues Mol. Biol.*, vol. 47, no. 6, p. 464, 2025.

[53] L. Kennedy, H. Francis, and G. Alpini, "Fructose promotion of intestinal and liver injury: A sugar by any other name that isn't so sweet," *Hepatology*, vol. 73, no. 6, pp. 2092–2094, 2021.

[54] T. Liu *et al.*, "Alcohol-metabolizing enzymes, liver diseases and cancer," in *Semin. Liver Dis.*. Thieme Medical Publishers, Inc., 2025.

[55] Y. Zhu, Y. Jia, and E. Zhang, "Oxidative stress modulation in alcohol-related liver disease: From Chinese botanical drugs to exercise-based interventions," *Front. Pharmacol.*, vol. 16, p. 1516603, 2025.

[56] S. G. E. Shams and R. G. Eissa, "Amelioration of ethanol-induced gastric ulcer in rats by quercetin: Implication of Nrf2/HO1 and HMGB1/TLR4/NF-κB pathways," *Heliyon*, vol. 8, no. 10, 2022.

[57] M. Raish *et al.*, "Gastroprotective effect of sinapic acid on ethanol-induced gastric ulcers in rats: Involvement of Nrf2/HO-1 and NF-κB signaling and antiapoptotic role," *Front. Pharmacol.*, vol. 12, p. 622815, 2021.

[58] C. A. Juan *et al.*, "The chemistry of reactive oxygen species (ROS) revisited: Outlining their role in biological macromolecules (DNA, lipids and proteins) and induced pathologies," *Int. J. Mol. Sci.*, vol. 22, no. 9, p. 4642, 2021.

[59] J. Hyun *et al.*, "Pathophysiological aspects of alcohol metabolism in the liver," *Int. J. Mol. Sci.*, vol. 22, no. 11, p. 5717, 2021.

[60] C. Bento *et al.*, "Striving for uniformity: A review on advances and challenges to achieve uniform polyethylene glycol," *Org. Process Res. Dev.*, vol. 28, no. 4, pp. 860–890, 2024.

[61] X. Li *et al.*, "Effects of flavonoids on alcoholic liver disease: A review," *Food Rev. Int.*, vol. 41, no. 1, pp. 173–200, 2025.

[62] K. R. LeFort, W. Rungratanawanich, and B.-J. Song, "Contributing roles of mitochondrial dysfunction and hepatocyte apoptosis in liver diseases through oxidative stress, post-translational modifications, inflammation, and intestinal barrier dysfunction," *Cell. Mol. Life Sci.*, vol. 81, no. 1, p. 34, 2024.

[63] D. Q. Huang *et al.*, "Global epidemiology of alcohol-associated cirrhosis and HCC: Trends, projections and risk factors," *Nat. Rev. Gastroenterol. Hepatol.*, vol. 20, no. 1, pp. 37–49, 2023.

[64] M. N. H. Malik *et al.*, "Geraniol suppresses oxidative stress, inflammation, and interstitial collagenase to protect against inflammatory arthritis," *ACS Omega*, vol. 8, no. 40, pp. 37128–37139, 2023.

[65] W. Zakiyah *et al.*, "Literature review: Study of molecular mechanism level of NSAID class of drugs as COX-2 inhibitors," *J. EduHealth*, vol. 13, no. 02, pp. 572–580, 2022.

[66] F. Kabir *et al.*, "Etoricoxib treatment prevented body weight gain and ameliorated oxidative stress in the liver of high-fat diet-fed rats," *Naunyn-Schmiedeberg's Arch. Pharmacol.*, vol. 394, pp. 33–47, 2021.

[67] S. Goswami *et al.*, "Gastroprotective potential of Indian medicinal plants—A comprehensive review," *Mathews J. Gastroenterol. Hepatol.*, vol. 9, no. 1, pp. 1–37, 2024.

[68] K. Rainsford, "Pharmacology and toxicology of ibuprofen," in *Ibuprofen: Discovery, Development and Therapeutics*. Wiley, 2015, pp. 132–236.

[69] G. Iolascon, S. Gimenez, and D. Mogyorosi, "A review of aceclofenac: Analgesic and anti-inflammatory effects on musculoskeletal disorders," *J. Pain Res.*, pp. 3651–3663, 2021.

[70] I. U. Umoh *et al.*, "Histomorphological and biochemical alterations on the liver of Wistar rats following co-administration of NSAIDs (piroxicam, diclofenac and ibuprofen)," *Anat. J. Africa*, vol. 11, no. 2, pp. 2175–2184, 2022.

[71] B. Mochahary, "Scientific validation of the formulation and evaluation of poly-herbal dosage for hepatoprotective active activity prescribed by the local medicinal practitioner of BTR, Assam, India," Ph.D. dissertation, Dept. Biotech., 2024.

[72] A. Tsoupras *et al.*, "The multifaceted effects of non-steroidal and non-opioid anti-inflammatory and analgesic drugs on platelets: Current knowledge, limitations, and future perspectives," *Pharmaceuticals*, vol. 17, no. 5, p. 627, 2024.

[73] Y. Macias *et al.*, "An update on the pharmacogenomics of NSAID metabolism and the risk of gastrointestinal bleeding," *Expert Opin. Drug Metab. Toxicol.*, vol. 16, no. 4, pp. 319–332, 2020.

[74] M. Li, C. Yu, and X. Zeng, "Comparative efficacy of traditional non-selective NSAIDs and selective cyclo-oxygenase-2 inhibitors in patients with acute gout: A systematic review and meta-analysis," *BMJ Open*, vol. 10, no. 9, p. e036748, 2020.

[75] N. Boby *et al.*, "Ethanol-induced hepatotoxicity and alcohol metabolism regulation by GABA-enriched fermented Smilax China root extract in rats," *Foods*, vol. 10, no. 10, p. 2381, 2021.

[76] A. B. Eason *et al.*, "DLX1008 (brolucizumab), a single-chain anti-VEGF-A antibody fragment with low picomolar affinity, leads to tumor involution in an in vivo model of Kaposi sarcoma," *PLoS One*, vol. 15, no. 5, p. e0233116, 2020.

[77] Y. Lei *et al.*, "A multicenter blinded preclinical randomized controlled trial on Jak1/2 inhibition in MRL/MpJ-Faslpr mice with proliferative lupus nephritis predicts low effect size," *Kidney Int.*, vol. 99, no. 6, pp. 1331–1341, 2021.

[78] A. Al Shoyaib, S. R. Archie, and V. T. Karamyan, "Intraperitoneal route of drug administration: Should it be used in experimental animal studies?" *Pharm. Res.*, vol. 37, no. 1, p. 12, 2020.

[79] H. Morris and R. Murray, "Healthcare, hygiene, and personal protective equipment (PPE)," in *Medical Textiles*. CRC Press, 2021, pp. 261–310.

[80] N. H. Shomer *et al.*, "Review of rodent euthanasia methods," *J. Amer. Assoc. Lab. Anim. Sci.*, vol. 59, no. 3, pp. 242–253, 2020.

[81] R. E. Meyer, "Euthanasia and humane killing," in *Veterinary Anesthesia and Analgesia: The Sixth Edition of Lumb and Jones*. Wiley, 2024, pp. 152–166.

[82] U. Aguwa, B. Obinwa, and C. Eze, "Histological effect of different inhalants on the heart and lungs of Wistar rats," *Asian J. Res. Cardiovasc. Dis.*, vol. 2, no. 3, pp. 27–35, 2020.

[83] C. Ramírez, "Lipids, chloroform, and their intertwined histories," *Substantia*, vol. 6, no. 1, pp. 133–143, 2022.

[84] U. Aguwa *et al.*, "Comparing the effect of methods of rat euthanasia on the brain of Wistar rats: Cervical dislocation, chloroform inhalation, diethyl ether inhalation and formalin inhalation," *J. Adv. Med. Med. Res.*, vol. 32, no. 17, pp. 8–1, 2020.

[85] E. J. Jo *et al.*, "Comparison of murine retroorbital plexus and facial vein blood collection to mitigate animal ethics issues," *Lab. Anim. Res.*, vol. 37, no. 1, p. 12, 2021.

[86] L. Charlès *et al.*, "Modified tail vein and penile vein puncture for blood sampling in the rat model," *J. Vis. Exp.*, no. 196, p. 10.3791/65513, 2023.

[87] F. Liang *et al.*, "Sevoflurane anaesthesia induces cognitive impairment in young mice through sequential tau phosphorylation," *Br. J. Anaesth.*, vol. 131, no. 4, pp. 726–738, 2023.

[88] W. Liang *et al.*, "Sulforaphane exerts beneficial immunomodulatory effects on liver tissue via a Nrf2 pathway-related mechanism in a murine model of hemorrhagic shock and resuscitation," *Front. Immunol.*, vol. 13, p. 822895, 2022.

[89] H. W. Liang *et al.*, "Mulberry leaves extract ameliorates alcohol-induced liver damages through reduction of acetaldehyde toxicity and inhibition of apoptosis caused by oxidative stress signals," *Int. J. Med. Sci.*, vol. 18, no. 1, pp. 53–64, 2021.

[90] I. Ates, "Investigating the potential of a cell-based gene editing therapy for inherited metabolic liver disease," Ph.D. dissertation, Clemson Univ., Clemson, SC, USA, 2023.

[91] R. A. Dop, D. R. Neill, and T. Hasell, "Sulfur-polymer nanoparticles: Preparation and antibacterial activity," *ACS Appl. Mater. Interfaces*, vol. 15, no. 17, pp. 20822–20832, 2023.

[92] M. J. Fecik *et al.*, "Voluntary wheel running exercise rescues behaviorally-evoked acetylcholine efflux in the medial prefrontal cortex and epigenetic changes in ChAT genes following adolescent intermittent ethanol exposure," *PLoS One*, vol. 19, no. 10, p. e0311405, 2024.

[93] U. Ullah *et al.*, "Hepatoprotective effects of melatonin and celecoxib against ethanol-induced hepatotoxicity in rats," *Immunopharmacol. Immunotoxicol.*, vol. 42, no. 3, pp. 255–263, 2020.